mathematics

MDPI

Article

Exploring the Dynamics of COVID-19 with a Novel Family of Models

Abdulaziz S. Alghamdi [1] and M. M. Abd El-Raouf [2,*]

[1] Department of Mathematics, College of Science & Arts, King Abdulaziz University, P.O. Box 344, Rabigh 21911, Saudi Arabia; ashalghamedi@kau.edu.sa
[2] Basic and Applied Science Institute, Arab Academy for Science, Technology and Maritime Transport (AASTMT), Alexandria P.O. Box 1029, Egypt
* Correspondence: m_abdelraouf85@aast.edu

Abstract: Much effort has recently been expended in developing efficient models that can depict the true picture for COVID-19 mortality data and help scientists choose the best-fit models. As a result, this research intends to provide a new G family for both theoretical and practical scientists that solves the concerns typically encountered in both normal and non-normal random events. The new-G distribution family is able to generate efficient continuous univariate and skewed models that may outperform the baseline model. The analytic properties of the new-G family and its sub-model are investigated and described, as well as a theoretical framework. The parameters were estimated using a classical approach along with an extensive simulation study to assess the behaviour of the parameters. The efficiency of the new-G family is discussed using one of its sub-models on COVID-19 mortality data sets.

Keywords: power function distribution; Rényi entropy; hazard rate function; Bonferroni and Lorenz curves; inference; COVID-19

MSC: 60E05

Citation: Alghamdi, A.S.; Abd El-Raouf, M.M. Exploring the Dynamics of COVID-19 with a Novel Family of Models. *Mathematics* **2023**, *11*, 1641. https://doi.org/10.3390/math11071641

Academic Editor: Maurizio Brizzi

Received: 11 January 2023
Revised: 15 March 2023
Accepted: 22 March 2023
Published: 28 March 2023

1. Introduction

Lifetime models are important for representing simple to complicated random occurrences, especially in the physical and natural sciences. In the statistical literature, many probability distributions are used to describe business failure data and are implemented in a diverse range of scenarios. Because of their established superiority in a number of contexts, gamma, lognormal, and Weibull distributions play an essential role. The one-parameter lifetime model, power function distribution (PFD), that occurs in several scientific disciplines and is a special case of uniform distribution. On the other side, the interest in the closed-form feature of PFD has grown and increased the curiosity of authors. Consequently, various generalizations and extensions have been previously established. For this, we urge the readers to look at the practices of Dallas [1], Saran and Pandey [2], Zaka et al. [3], Tahir et al. [4], Haq et al. [5], Okorie et al. [6], Hassan and Assar [7], and Meniconi and Barry [8], among others.

In several fields, actual data have been carefully modelled using a variety of classical distributions. To increase these distributions' flexibility and goodness of fit, however, there is often an obvious need for extended versions of them. As a consequence, generated families (G families) are established by modifying the baseline distribution by one or more additional shape parameters. Some of the well-known families recently developed by notable authors include: the Marshall–Olkin family generated by [9], QRTM by [10], Beta generated by [11], Gamma generated by [12], Kumaraswamy generated by [13], T-X family generated by [14], Weibull generated by [15], Type-I-Half-Logistic generated by [16], Topp–Leone generated by [17], and new power class by [18], to mention a few. Readers

who are interested in learning more about the COVID-19 mortality and the analysis are encouraged to refer to the work of Al-Babtain et al. [19], Liu et al. [20], Nagy et al. [21], Hossam et al. [22], Riad et al. [23], Alsuhabi et al. [24], and Meriem et al. [25].

In this scientific article, we are motivated to develop a simple and easy-to-understand new-G family that better depicts the complex nature of COVID-19 mortality events and assists scientists in selecting the most appropriate model. The flexible and attractive features of pdf and hrf are suitable for modelling an increasing, decreasing, upside-down bathtub-shaped failure rate and a wide range of data along with the events that are particularly associated with the COVID-19 pandemic issues in order to improve the characteristics of the baseline (parent) model and improve fit to data.

The present study is structured as follows. Section 2 presents some useful structural properties of the new family. Section 3 describes the analytical expressions and provides a graphical illustration of a new PFD. Section 4 estimates the parameters using classical techniques. Section 5 briefly illustrates the parameter behaviours based on an extensive simulation study. Section 6 describes the application of the proposed new-PFD to the COVID-19 mortality rate data along with a comparison with other well-known competitors. A summary and conclusions are stated in Section 7, and last, future recommendations are illustrated in Section 8.

2. The New Family of Distributions

New sub-models and corresponding baseline models see (Table 1)

Table 1. New sub-models and corresponding baseline models.

Model	Base Model	New Model
Exponential	$1-e^{-\beta x}$	$(1+\alpha)^{[1-e^{-\beta x}]}-\alpha^{[1-e^{-\beta x}]^2}\Big\vert_{\alpha,\beta>0}$
Weibull	$1-e^{-\beta x^{\gamma}}$	$(1+\alpha)^{[1-e^{-\beta x^{\gamma}}]}-\alpha^{[1-e^{-\beta x^{\gamma}}]^2}\Big\vert_{\alpha,\beta,\gamma>0}$
Rayleigh	$1-e^{-x^2/2\beta^2}$	$(1+\alpha)^{[1-e^{-x^2/2\beta^2}]}-\alpha^{[1-e^{-x^2/2\beta^2}]^2}\Big\vert_{\alpha,\beta,\gamma>0}$
Gompertz	$1-e^{-\beta(e^{\gamma x}-1)}$	$(1+\alpha)^{[1-e^{-\beta(e^{\gamma x}-1)}]}-\alpha^{[1-e^{-\beta(e^{\gamma x}-1)}]^2}\Big\vert_{\alpha,\beta,\gamma>0}$
Lomax	$1-[1+(x/\beta)]^{-\gamma}$	$(1+\alpha)^{[1-[1+(x/\beta)]^{-\gamma}]}-\alpha^{[1-[1+(x/\beta)]^{-\gamma}]^2}\Big\vert_{\alpha,\beta,\gamma>0}$
Burr	$1-\left[1+x^{\beta}\right]^{-\gamma}$	$(1+\alpha)^{[1-[1+x^{\beta}]^{-\gamma}]}-\alpha^{[1-[1+x^{\beta}]^{-\gamma}]^2}\Big\vert_{\alpha,\beta,\gamma>0}$
Pareto	$1-(x/x_{min})^{\gamma}$	$(1+\alpha)^{[1-(x/x_{min})^{\gamma}]}-\alpha^{[1-(x/x_{min})^{\gamma}]^2}\Big\vert_{\alpha,\gamma>0}$
Half Log-Logistic	$\left(1-e^{-\beta x}\right)/\left(1+e^{-\beta x}\right)$	$\left[(1+\alpha)^{[(1-e^{-\beta x})/(1+e^{-\beta x})]}-\alpha^{[(1-e^{-\beta x})/(1+e^{-\beta x})]^2}\right]\Big\vert_{\alpha,\beta>0}$
Kumaraswamy	$1-\left(1-x^{\beta}\right)^{\gamma}$	$(1+\alpha)^{[1-(1-x^{\beta})^{\gamma}]}-\alpha^{[1-(1-x^{\beta})^{\gamma}]^2}\Big\vert_{\alpha,\beta,\gamma>0}$
Power Function	$[x/M]^{\theta}$	$(1+\alpha)^{[x/M]^{\theta}}-\alpha^{[x/M]^{2\theta}}\Big\vert_{\alpha,\theta>0,M\geq x}$
Uniform	x/M	$(1+\alpha)^{[x/M]}-\alpha^{[x/M]^2}\Big\vert_{\alpha>0,M\geq x}$

Definition 1. *If $X \sim$ new-G $(x;\alpha,\Theta)$ with scale $(\alpha>0)$ and vector space (Θ), the cdf $(F|_{x;\Theta})$ of the new-G is presented as follows:*

$$F|_{x;\alpha,\Theta}=(1+\alpha)^{G|_{x;\Theta}}-\alpha^{[G|_{x;\Theta}]^2}\Big\vert_{\alpha>0,x\in\Re}. \quad (1)$$

Definition 2. *If X ~ new-G (x; α, Θ) with scale (α > 0) and vector space (Θ), the pdf ($f|_{x;\Theta}$) of the new-G is presented as follows:*

$$f|_{x;\alpha,\Theta} = \left. \mathrm{g}|_{x;\Theta}(1+\alpha)^{G|_{x;\Theta}} log(1+\alpha) - 2\,\mathrm{g}|_{x;\Theta}\, G|_{x;\Theta}\alpha^{[G|_{x;\Theta}]^2} log\alpha \right|_{\alpha>0, x\in\Re}. \quad (2)$$

Definition 3. *If X ~ new-G (x; α, Θ) with scale (α > 0) and vector space (Θ), the survival function ($sf|_{x;\Theta}$) of the new-G is presented as follows:*

$$sf|_{x;\alpha,\Theta} = \left. 1 - (1+\alpha)^{G|_{x;\Theta}} + \alpha^{[G|_{x;\Theta}]^2} \right|_{k>0, x\in\Re}. \quad (3)$$

Definition 4. *If X ~ new-G (x; α, Θ) with scale (α > 0) and vector space (Θ), the hazard rate function ($hrf|_{x;\alpha,\Theta}$) of the new-G is presented as follows:*

$$hrf|_{x;\alpha,\Theta} = \left. \frac{\mathrm{g}|_{x;\Theta}\left[(1+\alpha)^{G|_{x;\Theta}} log(1+\alpha) - 2\,G|_{x;\Theta}\alpha^{[G|_{x;\Theta}]^2} log\alpha\right]}{1 - (1+\alpha)^{G|_{x;\Theta}} + \alpha^{[G|_{x;\Theta}]^2}} \right|_{\alpha>0, x\in\Re}. \quad (4)$$

Definition 5. *If X ~ new-G (x; α, θ) with scale (α > 0) and vector space (Θ), r-th moments about origin (say $\mu'_r|_{x;\alpha,\Theta} = \int_{-\infty}^{+\infty} x^r f|_{x;\alpha,\Theta} dx$) is presented as follows:*

$$\mu'_r|_{x;\alpha,\Theta} = \sum_{l=0}^{\infty} \left. \begin{bmatrix} \frac{\{log(1+\alpha)\}^{l+1}}{l!} \int_{-\infty}^{+\infty} x^r\, \mathrm{g}|_{x;\Theta} \left\{ G|_{x;\Theta} \right\}^{l} dx - \\ 2\frac{\{log\alpha\}^{l+1}}{l!} \int_{-\infty}^{+\infty} x^r\, \mathrm{g}|_{x;\Theta} \left\{ G|_{x;\Theta} \right\}^{l+1} dx \end{bmatrix} \right|_{\alpha>0, x\in\Re}.$$

It would be more precise to say that $\mu'_r|_{x;\alpha,\Theta}$ is

$$\mu'_r|_{x;\alpha,\Theta} = \left. \sum_{l=0}^{\infty} \Phi|_{l+1}\, I|_{r,l} - 2\,\Phi|_{l+1}\, I|_{r,l+1} \right|_{\alpha>0, x\in\Re}$$

First incomplete moments ($\psi'_1|_{x;\alpha,\Theta}$), which might be more helpful in the discussion of Bonferroni and Lorenz curves, could be more conveniently derived with the assistance of $\mu'_r|_{x;\alpha,\Theta}$. Hence, $\psi'_1|_{x;\alpha,\Theta}$ can be presented as follows:

$$\psi'_1|_{x;\alpha,\Theta} = \left. \sum_{l=0}^{\infty} \Phi|_{l+1}\, I|_{1,t,l} - 2\,\Phi|_{l+1}\, I|_{1,t,l+1} \right|_{\alpha>0, x\in\Re}$$

where $I|_{r,l} = \int_{-\infty}^{+\infty} x^r\, \mathrm{g}|_{x;\Theta} \{ G|_{x;\Theta} \}^l dx$, $I|_{r,l+1} = \int_{-\infty}^{+\infty} x^r\, \mathrm{g}|_{x;\Theta} \{ G|_{x;\Theta} \}^{l+1} dx$, $I|_{1,t,l} = \int_{-\infty}^{t} x\, \mathrm{g}|_{x;\Theta} \{ G|_{x;\Theta} \}^l dx$, $I|_{1,t,l+1} = \int_{-\infty}^{t} x\, \mathrm{g}|_{x;\Theta} \{ G|_{x;\Theta} \}^{l+1} dx$, and $\Phi|_{l+1} = \frac{\{log(1+\alpha)\}^{l+1}}{l!}$.

It is important to keep in mind that the integrals may be computed numerically for the baseline models.

2.1. Asymptotics

The asymptotic for new-G $(x;\alpha,\Theta)$ cdf, pdf, sf, and hrf at $\lim_{x\to 0}$ and $\lim_{x\to\infty}$ are, respectively, presented as follows:

1-$\lim_{x\to 0} F|_{0;\alpha,\Theta} = 0$, and $\lim_{x\to\infty} F|_{\infty;\alpha,\Theta} = 1$.
2-$\lim_{x\to 0} f|_{0;\alpha,\Theta} = \mathrm{g}|_{x;\Theta} log(1+\alpha)$, and $\lim_{x\to\infty} f|_{\infty;\alpha,\Theta} = \mathrm{g}|_{x;\Theta}[(1+\alpha)log(1+\alpha) - 2\alpha log\alpha]$.
3-$\lim_{x\to 0} sf|_{0;\alpha,\Theta} = 1$, and $\lim_{x\to\infty} sf|_{\infty;\alpha,\Theta} = 0$.
4-$\lim_{x\to 0} hrf|_{0;\alpha,\Theta} = \mathrm{g}|_{x;\Theta} log(1+\alpha)$, and $\lim_{x\to\infty} hrf|_{\infty;\alpha,\Theta} =$ undefined.

2.2. Useful Representation

Mixture representation (MR) is very common and useful to discuss complex type characteristics of pdf and cdf. The cdf of new-G in terms of MR

$$F_{MR}|_{x;\alpha,\Theta} = \sum_{i=0}^{\infty}\left[\frac{\{log(1+\alpha)\}^i}{i!}\{G|_{x;\Theta}\}^i - \frac{\{log\alpha\}^i}{i!}[G|_{x;\Theta}]^{2i}\right]\Bigg|_{\alpha>0,x\in\Re},$$

and pdf are, respectively, presented as follows:

$$f_{MR}|_{x;\alpha,\Theta} = \mathrm{g}|_{x;\Theta}\sum_{l=0}^{\infty}\left[\frac{\{log(1+\alpha)\}^{l+1}}{l!}\{G|_{x;\Theta}\}^l - 2\frac{\{log\alpha\}^{l+1}}{l!}\{G|_{x;\Theta}\}^{l+1}\right]\Bigg|_{\alpha>0,x\in\Re}$$

2.3. Order Statistics (OS)

Suppose $X|_1, X|_2, X|_3, \ldots, X|_n$ are (iid) independent and identically distributed, random variables *(RVs)* from the new-G family of distributions. The pdf of the j-th OS $X|_{j:n}$ is presented by

$$f_{j:n}|_{x;\alpha,\Theta} = \frac{f|_{x;\alpha,\Theta}}{B(j,n-j+1)}\sum_{m=0}^{n-j}(-1)^m\binom{n-j}{m}[F|_{x;\alpha,\Theta}]^{m+j-1}.$$

One can easily determine the pdf of the j-th OS by placing the pertaining information into (1) and (2).

2.4. Entropy

This section gives a brief demonstration of the Rényi entropy measure (RE), the Tsallis entropy measure (TE), as well as the Havrda and Charvat entropy measure (HCE), all of which are formally derived in Sections 2.4.1–2.4.3, respectively.

2.4.1. Rényi Entropy

If $X \sim$ *new-G* $(x;\alpha,\Theta)$ with scale $(\alpha > 0)$ and vector space (Θ) the $RE|_{x;\alpha,\Theta}$ of the new-G is defined as follows:

$$RE|_{x;\alpha,\Theta} = \frac{1}{1-\Omega}log\int_{-\infty}^{+\infty}[f|_{x;\alpha,\Theta}]^{\Omega}dx. \tag{5}$$

By solving (2) in terms of Ω as

$$[f|_{x;\alpha,\Theta}]^{\Omega} = \left[\mathrm{g}|_{x;\Theta}(1+\alpha)^{G|_{x;\Theta}}log(1+\alpha) - 2\,\mathrm{g}|_{x;\Theta}\,G|_{x;\Theta}\alpha^{[G|_{x;\Theta}]^2}log\alpha\right]^{\Omega}\Bigg|_{\alpha,\Omega>0,\Omega\neq 1,x\in\Re}. \tag{6}$$

As we know all that in (6)

$$\mathrm{g}|_{x;\Theta}(1+\alpha)^{G|_{x;\Theta}}log(1+\alpha) > 2\,\mathrm{g}|_{x;\Theta}\,G|_{x;\Theta}\alpha^{[G|_{x;\Theta}]^2}log\alpha.$$

Hence, we consider the term $g|_{x;\Theta}(1+\alpha)^{G|_{x;\Theta}} log(1+\alpha)$ as common, and we get the simplified form of $[f|_{x;\alpha,\Theta}]^{\Omega}$ as

$$[f|_{x;\alpha,\Theta}]^{\Omega} = \left[\begin{matrix}\sum_{l_1=0}^{\infty}\binom{\Omega}{l_1}(-1)^{l_1}\left[2g|_{x;\Theta}G|_{x;\Theta}\alpha^{[G|_{x;\Theta}]^2}log\alpha\right]^{l_1}\times \\ [log(1+\alpha)g|_{x;\Theta}(1+\alpha)^{G|_{x;\Theta}}]^{\Omega-l_1}\end{matrix}\right]. \quad (7)$$

Now simplify,

$$\alpha^{l_1[G|_{x;\Theta}]^2} = e^{l_1[G|_{x;\Theta}]^2 log\alpha} = \sum_{l_2=0}^{\infty}\frac{[l_1 log\alpha]^{l_2}}{l_2!}[G|_{x;\Theta}]^{2l_2},$$

and

$$(1+\alpha)^{(\Omega-l_1)G|_{x;\Theta}} = e^{(\Omega-l_1)G|_{x;\Theta}log(1+\alpha)} = \sum_{l_3=0}^{\infty}\frac{[log(1+\alpha)]^{l_3}}{l_3!}(\Omega-l_1)^{l_3}[G|_{x;\Theta}]^{l_3}, \quad (8)$$

and substitute (8) into (7), we get

$$[f|_{x;\alpha,\Theta}]^{\Omega} = \sum_{l_1,l_2,l_3=0}^{\infty}\left[\begin{matrix}\binom{\Omega}{l_1}\frac{[l_1]^{l_2}[log(1+\alpha)]^{\Omega-l_1+l_3}}{l_2!l_3!} \\ [log(\alpha)]^{l_1+l_2}(-1)^{l_1}2^{l_1} \\ (\Omega-l_1)^{l_3}[g|_{x;\Theta}]^{\Omega}[G|_{x;\Theta}]^{l_1+2l_2+l_3}\end{matrix}\right]\Bigg|_{\alpha,\Omega>0,\Omega\neq1,x\in\Re}. \quad (9)$$

Hence, we get the final form of the $RE|_{x;\Theta}$ when (9) is placed into (5):

$$RE|_{x;\alpha,\Theta} = \frac{1}{1-\Omega}log\sum_{l_1,l_2,l_3=0}^{\infty}\left[\begin{matrix}\binom{\Omega}{l_1}\frac{[l_1]^{l_2}[log(1+\alpha)]^{\Omega-l_1+l_3}}{l_2!l_3!} \\ [log(\alpha)]^{l_1+l_2}(-1)^{l_1}2^{l_1} \\ (\Omega-l_1)^{l_3}[g|_{x;\Theta}]^{\Omega}[G|_{x;\Theta}]^{l_1+2l_2+l_3}\end{matrix}\right]\Bigg|_{\alpha,\Omega>0,\Omega\neq1,x\in\Re}.$$

2.4.2. Tsallis Entropy

If $X \sim$ *new-G* $(x;\alpha,\Theta)$ with scale $(\alpha>0)$ and vector space (Θ), the $TE|_{x;\alpha,\Theta}$ of the new-G is defined as follows:

$$TE|_{x;\alpha,\Theta} = \frac{1}{1-\Omega}\int_{-\infty}^{+\infty}[f|_{x;\Theta}]^{\Omega}dx - 1. \quad (10)$$

Hence, we get the final form of the $TE|_{x;\Theta}$ when (9) is placed into (10):

$$TE|_{x;\alpha,\Theta} = \frac{1}{1-\Omega}\sum_{l_1,l_2,l_3=0}^{\infty}\left[\begin{matrix}\binom{\Omega}{l_1}\frac{[l_1]^{l_2}[log(1+\alpha)]^{\Omega-l_1+l_3}}{l_2!l_3!} \\ [log(\alpha)]^{l_1+l_2}(-1)^{l_1}2^{l_1} \\ (\Omega-l_1)^{l_3}[g|_{x;\Theta}]^{\Omega}[G|_{x;\Theta}]^{l_1+2l_2+l_3}\end{matrix}\right]-1\Bigg|_{\alpha,\Omega>0,\Omega\neq1,x\in\Re}.$$

2.4.3. Havrda and Charvat Entropy

If $X \sim$ *new-G* $(x;\alpha,\Theta)$ with scale $(\alpha>0)$ and vector space (Θ), the $HCE|_{x;\alpha,\Theta}$ of the new-G is defined as follows:

$$HCE|_{x;\alpha,\Theta} = \frac{1}{2^{1-\Omega}-1}\int_{-\infty}^{+\infty}[f|_{x;\Theta}]^{\Omega}dx - 1. \quad (11)$$

Hence, we get the final form of the $HCE|_{x;\Theta}$ when (9) is placed into (11):

$$HCE|_{x;\alpha,\Theta} = A \sum_{l_1,l_2,l_3=0}^{\infty} \left[\begin{array}{c} \binom{\Omega}{l_1} \frac{[l_1]^{l_2}[log(1+\alpha)]^{\Omega-l_1+l_3}}{l_2!l_3!} \\ [log(\alpha)]^{l_1+l_2}(-1)^{l_1}2^{l_1} \\ (\Omega-l_1)^{l_3}[g|_{x;\Theta}]^{\Omega}[G|_{x;\Theta}]^{l_1+2l_2+l_3} \end{array} \right] - 1 \Bigg|_{\alpha,\Omega>0,\Omega\neq1,x\in\Re},$$

where $A = \frac{1}{2^{1-\Omega}-1}$.

2.5. Inference

Let $X_j \sim$ *new-G* $(x_j;\alpha,\Theta)$ with scale $(\alpha > 0)$ and vector space $(\Theta)^T$, then the log-likelihood $l(\Theta)$ from a random sample of size n is given by

$$l_{\vartheta}|_{x;\alpha,\Theta} = \sum_{j=1}^{n} log[g|_{x;\Theta}] + \sum_{j=1}^{n} log\left[(1+\alpha)^{G|_{x;\Theta}} log(1+\alpha) - 2G|_{x;\Theta}\alpha^{[G|_{x;\Theta}]^2} log\alpha\right]\Big|_{\alpha>0,x\in\Re}. \quad (12)$$

The ML estimator $\vartheta = (\alpha,\Theta)^T$ can be derived by maximizing the $l_{\vartheta}|_{x;\Theta}$ or solving the nonlinear likelihood equations simultaneously by differentiating (12). The partial derivative of $l_{\vartheta}|_{x;\Theta}$ is provided in the following form for both α and Θ, respectively:

$$\frac{\partial l_{\vartheta}|_{x;\alpha,\Theta}}{\partial\alpha} = \left[\frac{1}{p|_1 - p|_2}\right]\left[\frac{(1+\alpha)^{G|_{x;\Theta}}}{(1+\alpha)} + \{log(1+\alpha)\}^2(1+\alpha)^{G|_{x;\Theta}}\right],$$

$$\frac{\partial l_{\vartheta}|_{x;\alpha,\Theta}}{\partial\Theta} = \left[\frac{1}{p|_1 - p|_2}\right]\sum_{j=1}^{n}\left[\{log(1+\alpha)\}^2(1+\alpha)^{G|_{x;\Theta}} - 2log\alpha\left[1+2\{G|_{x;\Theta}\}^2 log\alpha\right]\frac{\partial G|_{x;\Theta}}{\partial\Theta}\right],$$

where $p|_1 = (1+\alpha)^{G|_{x;\Theta}} log(1+\alpha)$ and $p|_2 = 2G|_{x;\Theta}\alpha^{[G|_{x;\Theta}]^2} log\alpha$.

3. Mathematical Characteristics of Sub-Model

The PFD, which has cdf $[x/M]^{\theta}$ and pdf $[\theta/M][x/M]^{\theta-1}, \theta > 0, M \geq x$, is a well-known simple function with powerful characteristics, and is consider for detailed discussion in this section. The cdf, pdf, sf, and hrf of the new-PFD can be illustrated, respectively, as follows:

$$F|_x = (1+\alpha)^{[\frac{x}{M}]^{\theta}} - \alpha^{[\frac{x}{M}]^{2\theta}}\Big|_{k,\theta>0,M\geq x}, \quad (13)$$

$$f|_x = \left[\frac{\theta}{M}\right]\left[\frac{x}{M}\right]^{\theta-1}\left[(1+\alpha)^{[\frac{x}{M}]^{\theta}} log(1+\alpha) - 2\left[\frac{x}{M}\right]^{\theta}\alpha^{[\frac{x}{M}]^{2\theta}} log\alpha\right]\Big|_{\alpha,\theta>0,M\geq x}, \quad (14)$$

$$sf|_x = 1 - (1+\alpha)^{[\frac{x}{M}]^{\theta}} + \alpha^{[\frac{x}{M}]^{2\theta}}\Big|_{\alpha,\theta>0,M\geq x}, \quad (15)$$

$$hrf|_x = \frac{\left[\frac{\theta}{M}\right]\left[\frac{x}{M}\right]^{\theta-1}\left[(1+\alpha)^{[\frac{x}{M}]^{\theta}} log(1+\alpha) - 2\left[\frac{x}{M}\right]^{\theta}\alpha^{[\frac{x}{M}]^{2\theta}} log\alpha\right]}{1-(1+\alpha)^{[\frac{x}{M}]^{\theta}} + \alpha^{[\frac{x}{M}]^{2\theta}}}\Bigg|_{\alpha,\theta>0,M\geq x}. \quad (16)$$

3.1. Useful Representation

The MR, which is developed for pdf of the new-PFD, will be very useful for deriving moments and other characteristics. The analytical expression of the MR is presented as follows:

$$f_{MR}|_x = \sum_{l=0}^{\infty}\left[\begin{array}{c} \frac{\{log(1+\alpha)\}^{l+1}}{l!}\left\{\frac{\theta}{M^{\theta+l(\theta-1)}}\right\}x^{(\theta-1)(l+1)} - \\ 2\frac{\{log\alpha\}^{l+1}}{l!}\left\{\frac{\theta}{M^{\theta+(l+1)(\theta-1)}}\right\}x^{(\theta-1)(l+2)} \end{array}\right]\Bigg|_{\alpha,\theta>0,M\geq x}. \quad (17)$$

3.2. Moments and Related Measures

Theorem 1. *If $X \sim$ new-PFD $(x;\alpha,\theta)$ with $\alpha,\theta > 0$ and $M \geq x$, r-th moments about origin (say $\mu'_r|_x$) is presented as follows:*

$$\mu'_r|_x = \sum_{l=0}^{\infty}\left[\theta M^r\left\{\frac{\{log(1+\alpha)\}^{l+1}}{l!\{(r+\theta)+l(\theta-1)\}} - \frac{2\{log\alpha\}^{l+1}}{l!\{(r+1)+(\theta-1)(l+2)\}}\right\}\right]\Bigg|_{\alpha,\theta>0,M\geq x}.$$

Proof. The $\mu'_r|_x$ is denoted by

$$\mu'_r|_x = \int_0^M x^r f|_x dx.$$

By substituting the analytical expression from (17), we get

$$\mu'_r|_x = \int_0^M x^r \sum_{l=0}^{\infty}\left[\begin{array}{l}\frac{\{log(1+\alpha)\}^{l+1}}{l!}\left\{\frac{\theta}{M^{\theta+l(\theta-1)}}\right\}x^{(\theta-1)(l+1)} - \\ 2\frac{\{log\alpha\}^{l+1}}{l!}\left\{\frac{\theta}{M^{\theta+(l+1)(\theta-1)}}\right\}x^{(\theta-1)(l+2)}\end{array}\right]dx\Bigg|_{\alpha,\theta>0,M\geq x}.$$

The last expression of $\mu'_r|_x$ can be expressed as follows:

$$\mu'_r|_x = \sum_{j=0}^{\infty}\left[\begin{array}{l}\frac{\{log(1+\alpha)\}^{l+1}}{l!}\left\{\frac{\theta}{M^{\theta+l(\theta-1)}}\right\}\int_0^M x^{r+(\theta-1)(l+1)}dx - \\ 2\frac{\{log\alpha\}^{l+1}}{l!}\left\{\frac{\theta}{M^{\theta+(l+1)(\theta-1)}}\right\}\int_0^M x^{(\theta-1)(l+2)}dx\end{array}\right]\Bigg|_{\alpha,\theta>0,M\geq x}.$$

Here, we explore all possible shapes that the new-PFD may have for different combinations of parameters. Figure 1 shows all of the pdf curves that are possible and Figure 2 presents the flexible shapes that clearly depict the increasing and bathtub-shaped curves of hrf.

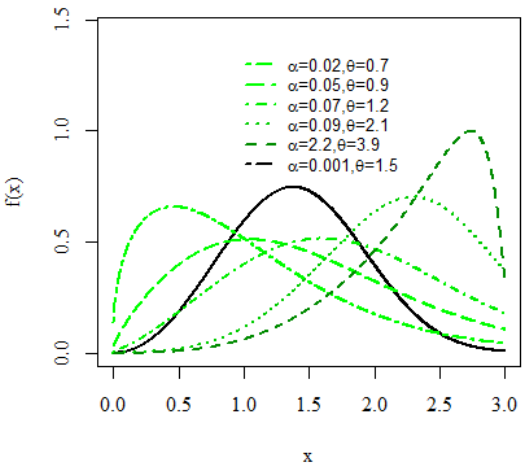

Figure 1. PDF plots for different parameter combinations.

By applying simple mathematics to the last expression, we get the final analytical expression of the *r*-th moments about the origin of the new-PFD and it is presented as follows:

$$\mu'_r|_x = \sum_{l=0}^{\infty}\left[\theta M^r\left\{\frac{\{log(1+\alpha)\}^{l+1}}{l!\{(r+\theta)+l(\theta-1)\}} - \frac{2\{log\alpha\}^{l+1}}{l!\{(r+1)+(\theta-1)(l+2)\}}\right\}\right]\Bigg|_{\alpha,\theta>0,M\geq x}. \quad (18)$$

□

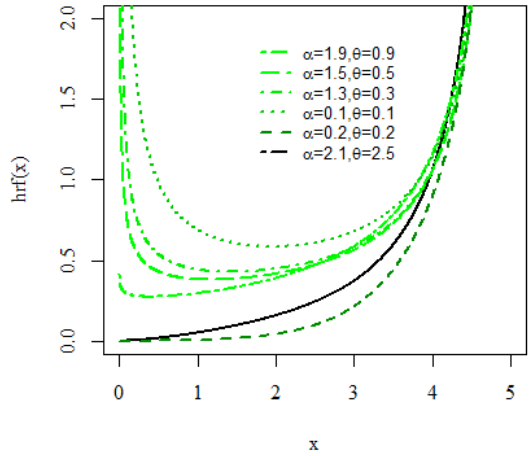

Figure 2. HRF plots for different parameter combinations.

Corollary 1. *By placing r = 1,2,3,4,-v, and −1 in (18), we get the 1st four moments (say* $\mu'_1|_x$, $\mu'_2|_x$, $\mu'_3|_x$, $\mu'_4|_x$*), negative moments (say* $\mu'_{-v}|_x$*), harmonic mean (say* $\mu'_{-1}|_x$*), and variance (*$Var|_x$*) of the new-PFD and the analytical expressions are, respectively, presented as follows:*

$$\mu'_1|_x = \sum_{l=0}^{\infty}\left[\theta M\left\{\frac{\{log(1+\alpha)\}^{l+1}}{l!\{(1+\theta)+l(\theta-1)\}} - \frac{2\{log\alpha\}^{l+1}}{l!\{2+(\theta-1)(l+2)\}}\right\}\right]\Bigg|_{\alpha,\theta>0,M\geq x},$$

$$\mu'_2|_x = \sum_{l=0}^{\infty}\left[\theta M^2\left\{\frac{\{log(1+\alpha)\}^{l+1}}{l!\{(2+\theta)+l(\theta-1)\}} - \frac{2\{log\alpha\}^{l+1}}{l!\{3+(\theta-1)(l+2)\}}\right\}\right]\Bigg|_{\alpha,\theta>0,M\geq x},$$

$$\mu'_3|_x = \sum_{l=0}^{\infty}\left[\theta M^3\left\{\frac{\{log(1+\alpha)\}^{l+1}}{l!\{(3+\theta)+l(\theta-1)\}} - \frac{2\{log\alpha\}^{l+1}}{l!\{4+(\theta-1)(l+2)\}}\right\}\right]\Bigg|_{\alpha,\theta>0,M\geq x},$$

$$\mu'_4|_x = \sum_{l=0}^{\infty}\left[\theta M^4\left\{\frac{\{log(1+\alpha)\}^{l+1}}{l!\{(4+\theta)+l(\theta-1)\}} - \frac{2\{log\alpha\}^{l+1}}{l!\{4+(\theta-1)(l+2)\}}\right\}\right]\Bigg|_{\alpha,\theta>0,M\geq x},$$

$$\mu'_{-v}|_x = \sum_{l=0}^{\infty}\left[\frac{\theta}{M^v}\left\{\frac{\{log(1+\alpha)\}^{l+1}}{l!\{(\theta-v)+l(\theta-1)\}} - \frac{2\{log\alpha\}^{l+1}}{l!\{(1-v)+(\theta-1)(l+2)\}}\right\}\right]\Bigg|_{\alpha,\theta>0,M\geq x},$$

$$\mu'_{-1}|_x = \sum_{l=0}^{\infty}\left[\frac{\theta}{M}\left\{\frac{\{log(1+\alpha)\}^{l+1}}{l!\{(\theta-1)+l(\theta-1)\}} - \frac{2\{log\alpha\}^{l+1}}{l!\{(\theta-1)(l+2)\}}\right\}\right]\Bigg|_{\alpha,\theta>0,M\geq x},$$

$$Var|_x = \left.\begin{array}{l}\sum_{l=0}^{\infty}\left[\theta M^2\left\{\frac{\{log(1+\alpha)\}^{l+1}}{l!\{(2+\theta)+l(\theta-1)\}} - \frac{2\{log\alpha\}^{l+1}}{l!\{3+(\theta-1)(l+2)\}}\right\}\right] - \\ \left[\sum_{l=0}^{\infty}\left[\theta M\left\{\frac{\{log(1+\alpha)\}^{l+1}}{l!\{(1+\theta)+l(\theta-1)\}} - \frac{2\{log\alpha\}^{l+1}}{l!\{2+(\theta-1)(l+2)\}}\right\}\right]\right]^2\end{array}\right|_{\alpha,\theta>0,M\geq x}.$$

It is worth noting that $\mu_2|_x = \mu'_2|_x - \mu'_1|_x^2$; $\mu_3|_x = 2\mu'_1|_x^3 - 3\mu'_2|_x\mu'_1|_x - \mu'_3|_x$; *and* $\mu_4|_x = \mu'_4|_x - 3\mu'_1|_x^4 + 6\mu'_1|_x^2\mu'_2|_x - 4\mu'_3|_x\mu'_1|_x$. *Furthermore, the coefficient of skewness and coefficient of kurtosis is easily determined by* $\tau_1|_x = \frac{\mu'_3|_x^2}{\mu'_2|_x^3}$ *and* $\tau_2|_x = \frac{\mu_4|_x}{\mu'_2|_x^2}$, *respectively.*

Theorem 2. *If X ~ new-PFD* $(x;\alpha,\theta)$ *with* $\alpha,\theta>0$ *and* $M\geq x$, *the moment generating function (say* $MGF|_x$*) is presented as follows:*

$$MGF|_x = \sum_{r=0}^{\infty} \frac{t^r}{r!} \sum_{l=0}^{\infty} \left[\theta M^r \left\{ \frac{\{log(1+\alpha)\}^{l+1}}{l!\{(r+\theta)+l(\theta-1)\}} - \frac{2\{log\alpha\}^{l+1}}{l!\{(r+1)+(\theta-1)(l+2)\}} \right\} \right] \Bigg|_{\alpha,\theta>0,M\geq x}.$$

Proof. The $MGF|_x$ is denoted by

$$MGF|_x = \int_0^M e^{tx} f|_x dx.$$

By following (17),

$$MGF|_x = \int_0^M e^{tx} \sum_{l=0}^{\infty} \left[\begin{array}{l} \frac{\{log(1+\alpha)\}^{l+1}}{l!} \left\{ \frac{\theta}{M^{\theta+l(\theta-1)}} \right\} x^{(\theta-1)(l+1)} - \\ 2\frac{\{log\alpha\}^{l+1}}{l!} \left\{ \frac{\theta}{M^{\theta+(l+1)(\theta-1)}} \right\} x^{(\theta-1)(l+2)} \end{array} \right] dx \Bigg|_{\alpha,\theta>0,M\geq x}.$$

We can write $e^{tx} as \sum_{r=0}^{\infty} (t^r/r!)x^r$. Hence, by following (17), $MGF|_x$ of the new-PFD is derived after applying a few mathematical steps, and the analytical expression of $MGF|_x$ can be presented as follows:

$$MGF|_x = \sum_{r=0}^{\infty} \frac{t^r}{r!} \sum_{l=0}^{\infty} \left[\theta M^r \left\{ \frac{\{log(1+\alpha)\}^{l+1}}{l!\{(r+\theta)+l(\theta-1)\}} - \frac{2\{log\alpha\}^{l+1}}{l!\{(r+1)+(\theta-1)(l+2)\}} \right\} \right] \Bigg|_{\alpha,\theta>0,M\geq x}.$$

□

Theorem 3. *If X ~ new-PFD (x; α, θ) with α, θ > 0 and M ≥ x, the characteristic function (say $CF|_x$) is presented as follows:*

$$CF|_x = \sum_{r=0}^{\infty} \frac{(it)^r}{r!} \sum_{l=0}^{\infty} \left[\theta M^r \left\{ \frac{\{log(1+\alpha)\}^{l+1}}{l!\{(r+\theta)+l(\theta-1)\}} - \frac{2\{log\alpha\}^{l+1}}{l!\{(r+1)+(\theta-1)(l+2)\}} \right\} \right] \Bigg|_{\alpha,\theta>0,M\geq x}.$$

Proof. The $CF|_x$ is denoted by

$$CF|_x = \int_0^M e^{itx} f|_x dx.$$

By following (17),

$$CF|_x = \int_0^M e^{itx} \sum_{l=0}^{\infty} \left[\begin{array}{l} \frac{\{log(1+\alpha)\}^{l+1}}{l!} \left\{ \frac{\theta}{M^{\theta+l(\theta-1)}} \right\} x^{(\theta-1)(l+1)} - \\ 2\frac{\{log\alpha\}^{l+1}}{l!} \left\{ \frac{\theta}{M^{\theta+(l+1)(\theta-1)}} \right\} x^{(\theta-1)(l+2)} \end{array} \right] dx \Bigg|_{\alpha,\theta>0,M\geq x}.$$

We can write $e^{itx} as \sum_{r=0}^{\infty} \left[(it)^r/r!\right] x^r$. Hence, by following (17), $CF|_x$ of the new-PFD is derived after applying a few mathematical steps, and the analytical expression of $CF|_x$ can be presented as follows:

$$CF|_x = \sum_{r=0}^{\infty} \frac{(it)^r}{r!} \sum_{l=0}^{\infty} \left[\theta M^r \left\{ \frac{\{log(1+\alpha)\}^{l+1}}{l!\{(r+\theta)+l(\theta-1)\}} - \frac{2\{log\alpha\}^{l+1}}{l!\{(r+1)+(\theta-1)(l+2)\}} \right\} \right] \Bigg|_{\alpha,\theta>0,M\geq x}.$$

□

Theorem 4. *If $X \sim$ new-PFD $(x;\alpha,\theta)$ with $\alpha,\theta>0$ and $M \geq x$, the Millan transformation (say $MT|_x$) is presented as follows:*

$$MT|_x = \sum_{l=0}^{\infty}\left[\theta M^{y-1}\left\{\frac{\{log(1+\alpha)\}^{l+1}}{l!\{(y-1+\theta)+l(\theta-1)\}} - \frac{2\{log\alpha\}^{l+1}}{l!\{y+(\theta-1)(l+2)\}}\right\}\right]\Bigg|_{\alpha,\theta>0,M\geq x}.$$

Proof. The $MT|_x$ is denoted by

$$MT|_x = \int_0^M x^{y-1} f|_x dx.$$

By following (17),

$$MT|_x = \int_0^M x^{y-1}\sum_{l=0}^{\infty}\left[\begin{array}{l}\frac{\{log(1+\alpha)\}^{l+1}}{l!}\left\{\frac{\theta}{M^{\theta+l(\theta-1)}}\right\}x^{(\theta-1)(l+1)} - \\ 2\frac{\{log\alpha\}^{l+1}}{l!}\left\{\frac{\theta}{M^{\theta+(l+1)(\theta-1)}}\right\}x^{(\theta-1)(l+2)}\end{array}\right]dx\Bigg|_{\alpha,\theta>0,M\geq x}.$$

We can describe $MT|_x$ of the new-PFD after applying a few mathematical steps, and the analytical expression of $MT|_x$ can be presented as follows:

$$\mu'_{MT}\Big|_x = \sum_{l=0}^{\infty}\left[\theta M^{y-1}\left\{\frac{\{log(1+\alpha)\}^{l+1}}{l!\{(y-1+\theta)+l(\theta-1)\}} - \frac{2\{log\alpha\}^{l+1}}{l!\{y+(\theta-1)(l+2)\}}\right\}\right]\Bigg|_{\alpha,\theta>0,M\geq x}.$$

□

Theorem 5. *If $X \sim$ new-PFD $(x;\alpha,\theta)$ with $\alpha,\theta>0$ and $M \geq x$, the harmonic mean (say $HM|_x$) is presented as follows:*

$$HM|_x = \sum_{l=0}^{\infty}\left[\frac{\theta}{M}\left\{\frac{\{log(1+\alpha)\}^{l+1}}{l!\{(r+\theta)+l(\theta-1)\}} - \frac{2\{log\alpha\}^{l+1}}{l!\{(r+1)+(\theta-1)(l+2)\}}\right\}\right]\Bigg|_{\alpha,\theta>0,M\geq x}.$$

Proof. The $HM|_x$ is denoted by

$$HM|_x = \int_0^M (1/x) f|_x dx.$$

By following (17),

$$HM|_x = \int_0^M (1/x)\sum_{l=0}^{\infty}\left[\begin{array}{l}\frac{\{log(1+\alpha)\}^{l+1}}{l!}\left\{\frac{\theta}{M^{\theta+l(\theta-1)}}\right\}x^{(\theta-1)(l+1)} - \\ 2\frac{\{log\alpha\}^{l+1}}{l!}\left\{\frac{\theta}{M^{\theta+(l+1)(\theta-1)}}\right\}x^{(\theta-1)(l+2)}\end{array}\right]dx\Bigg|_{\alpha,\theta>0,M\geq x}.$$

We can describe $HM|_x$ of the new-PFD after applying a few mathematical steps, and the analytical expression of $HM|_x$ can be presented as follows:

$$HM|_x = \sum_{l=0}^{\infty}\left[\frac{\theta}{M}\left\{\frac{\{log(1+\alpha)\}^{l+1}}{l!\{(\theta-1)+l(\theta-1)\}} - \frac{2\{log\alpha\}^{l+1}}{l!\{(\theta-1)(l+2)\}}\right\}\right]\Bigg|_{\alpha,\theta>0,M\geq x}.$$

□

Theorem 6. *If $X \sim$ new-PFD $(x;\alpha,\theta)$ with $\alpha,\theta > 0$ and $M \geq x$, the p-th incomplete moment (say $ICM|_p$) is presented as follows:*

$$ICM|_p = \sum_{l=0}^{\infty}\left[\frac{\theta}{t}\left\{\frac{\{log(1+\alpha)\}^{l+1}}{l!\{(p+\theta)+l(\theta-1)\}} - \frac{2\{log\alpha\}^{l+1}}{l!\{(p+1)+(\theta-1)(l+2)\}}\right\}\right]\Bigg|_{\alpha,\theta>0,M\geq x}.$$

Proof. The $ICM|_p$ is denoted by

$$ICM|_p = \int_0^t x^p f|_x dx.$$

By following (17),

$$ICM|_p = \int_0^t x^p \sum_{l=0}^{\infty}\left[\begin{array}{c}\frac{\{log(1+\alpha)\}^{l+1}}{l!}\left\{\frac{\theta}{M^{\theta+l(\theta-1)}}\right\}x^{(\theta-1)(l+1)} - \\ 2\frac{\{log\alpha\}^{l+1}}{l!}\left\{\frac{\theta}{M^{\theta+(l+1)(\theta-1)}}\right\}x^{(\theta-1)(l+2)}\end{array}\right]dx\Bigg|_{\alpha,\theta>0,M\geq x}.$$

We can describe $ICM|_p$ of the new-PFD after applying a few mathematical steps, and the analytical expression of $ICM|_p$ can be presented as follows:

$$ICM|_p = \left[\theta t^p\left\{\frac{\{log(1+\alpha)\}^{l+1}}{l!\{(r+\theta)+l(\theta-1)\}} - \frac{2\{log\alpha\}^{l+1}}{l!\{(r+1)+(\theta-1)(l+2)\}}\right\}\right]\Bigg|_{\alpha,\theta>0,M\geq x}.$$

□

Corollary 2. *By placing p = 1 in $ICM|_p$ (last expression), we get the 1st incomplete moment (say $ICM|_1$) of the new-PFD and the analytical expression is presented as follows:*

$$ICM|_1 = \sum_{l=0}^{\infty}\left[\theta t\left\{\frac{\{log(1+\alpha)\}^{l+1}}{l!\{(r+\theta)+l(\theta-1)\}} - \frac{2\{log\alpha\}^{l+1}}{l!\{(r+1)+(\theta-1)(l+2)\}}\right\}\right]\Bigg|_{\alpha,\theta>0,M\geq x}.$$

It is worth noting that the Bonferroni and Lorenz curves have major implementation in $ICM|_1$ and they are well-defined as $B|_p = ICM_t|_1/\mu_1'|_x$ and $L|_p = ICM_p|_1/p\mu_1'|_x$, respectively. There are many applications for these curves in fields such as economics, demography, insurance, engineering, and medicine. Mean residual life and mean waiting time (see Section 3.3.1) are two further examples of contexts in which the first incomplete instant is useful.

Theorem 7. *If $X \sim$ new-PFD $(x;\alpha,\theta)$ with $\alpha,\theta > 0$ and $M \geq x$, the vitality function (say $VT|_x$) is presented as follows:*

$$VT|_x = \frac{1}{sf|_x}\left[\sum_{l=0}^{\infty}\left[\left\{\frac{\{log(1+\alpha)\}^{l+1}}{l!\{(1+\theta)+l(\theta-1)\}} - \frac{2\{log\alpha\}^{l+1}}{l!\{2+(\theta-1)(l+2)\}}\right\}\theta(M-x)\right]\right]\Bigg|_{\alpha,\theta>0,M\geq x}.$$

Proof. The $VT|_x$ is denoted by

$$VT|_x = \frac{1}{sf|_x}\int_x^M x f|_x dx.$$

By following (17),

$$VT|_x = \frac{1}{sf|_x}\int_x^M x\sum_{l=0}^{\infty}\left[\begin{array}{c}\frac{\{log(1+\alpha)\}^{l+1}}{l!}\left\{\frac{\theta}{M^{\theta+l(\theta-1)}}\right\}x^{(\theta-1)(l+1)}- \\ 2\frac{\{log\alpha\}^{l+1}}{l!}\left\{\frac{\theta}{M^{\theta+(l+1)(\theta-1)}}\right\}x^{(\theta-1)(l+2)}\end{array}\right]dx\Bigg|_{\alpha,\theta>0,M\geq x}.$$

We can describe $VT|_x$ of the new-PFD after applying a few mathematical steps, and the analytical expression of $VT|_x$ can be presented as follows:

$$VT|_x = \frac{1}{sf|_x}\left[\sum_{l=0}^{\infty}\left[\left\{\frac{\{log(1+\alpha)\}^{l+1}}{l!\{(1+\theta)+l(\theta-1)\}}-\frac{2\{log\alpha\}^{l+1}}{l!\{2+(\theta-1)(l+2)\}}\right\}\theta(M-x)\right]\right]\Bigg|_{\alpha,\theta>0,M\geq x}.$$

□

Theorem 8. *If $X \sim$ new-PFD $(x;\alpha,\theta)$ with $\alpha,\theta > 0$ and $M \geq x$, conditional moments (say $CM_x|_{x>v}$) are presented as follows:*

$$CM_x|_{x>v} = \frac{1}{sf|_v}\left[\sum_{l=0}^{\infty}\left[\left\{\frac{\{log(1+\alpha)\}^{l+1}}{l!\{(1+\theta)+l(\theta-1)\}}-\frac{2\{log\alpha\}^{l+1}}{l!\{2+(\theta-1)(l+2)\}}\right\}\theta(M-x)\right]\right]\Bigg|_{\alpha,\theta>0,M\geq x}.$$

Proof. The $CM_x|_{x>v}$ is denoted by

$$CM_x|_{x>v} = \frac{1}{sf|_v}\int_v^M x^r f|_x dx.$$

By following (17),

$$CM_x|_{x>v} = \frac{1}{sf|_v}\int_v^M x^r\sum_{l=0}^{\infty}\left[\begin{array}{c}\frac{\{log(1+\alpha)\}^{l+1}}{l!}\left\{\frac{\theta}{M^{\theta+l(\theta-1)}}\right\}x^{(\theta-1)(l+1)}- \\ 2\frac{\{log\alpha\}^{l+1}}{l!}\left\{\frac{\theta}{M^{\theta+(l+1)(\theta-1)}}\right\}x^{(\theta-1)(l+2)}\end{array}\right]dx\Bigg|_{\alpha,\theta>0,M\geq x}.$$

We can describe $CM_x|_{x>v}$ of the new-PFD after applying a few mathematical steps, and the analytical expression of $CM_x|_{x>v}$ can be presented as follows:

$$CM_x|_{x>v} = \frac{1}{sf|_v}\sum_{l=0}^{\infty}\left[\begin{array}{c}\left\{\frac{\{log(1+\alpha)\}^{l+1}}{l!\{(r+\theta)+l(\theta-1)\}}-\frac{2\{log\alpha\}^{l+1}}{l!\{(r+1)+(\theta-1)(l+2)\}}\right\}\times \\ \theta(M^r-v^r)\end{array}\right]\Bigg|_{\alpha,\theta>0,M\geq x}.$$

□

3.3. Residuals and Related Measures

Residual function (say RL) and reverse RL of the new-PFD is described as $R_w|_x = S(x+w)/S(w)|_{\alpha,\theta>0,M\geq x}$ and $\bar{R}_w|_x = S(x-w)/S(w)|_{\alpha,\theta>0,M\geq x}$, respectively. The analytical expressions are, respectively, presented as follows:

$$R_w|_x = 1-(1+\alpha)^{\left[\frac{x+w}{M}\right]^{\theta}}+\alpha^{\left[\frac{x+w}{M}\right]^{2\theta}}\Bigg|_{\alpha,\theta>0,M\geq x},$$

$$\bar{R}_w|_x = 1-(1+\alpha)^{\left[\frac{x-w}{M}\right]^{\theta}}+\alpha^{\left[\frac{x-w}{M}\right]^{2\theta}}\Bigg|_{\alpha,\theta>0,M\geq x}.$$

3.3.1. Mean Residual and Mean Inactivity Time

Mean RL and mean inactivity time (MIT) of the new-PFD are described as: $MRL_w|_x = \frac{1-ICM|_1}{S(w)-w}\Big|_{\alpha,\theta>0,M\geq x}$ and $MIT_w|_x = w - \frac{ICM|_1}{F(w)}\Big|_{\alpha,\theta>0,M\geq x}$, respectively, and are presented as follows:

$$MRL_w|_x = \left.\frac{1-\sum_{l=0}^{\infty}\left[\frac{\theta}{t}\left\{\frac{\{log(1+\alpha)\}^{l+1}}{l!\{(1+\theta)+l(\theta-1)\}}-\frac{2\{log\alpha\}^{l+1}}{l!\{2+(\theta-1)(l+2)\}}\right\}\right]}{S(w)-w}\right|_{\alpha,\theta>0,M\geq x},$$

$$MIT_w|_x = w - \left.\frac{\sum_{l=0}^{\infty}\left[\frac{\theta}{t}\left\{\frac{\{log(1+\alpha)\}^{l+1}}{l!\{(1+\theta)+l(\theta-1)\}}-\frac{2\{log\alpha\}^{l+1}}{l!\{2+(\theta-1)(l+2)\}}\right\}\right]}{F(w)}\right|_{\alpha,\theta>0,M\geq x}.$$

3.4. Entropy

This section gives a brief demonstration of the Rényi entropy measure (RE), the Tsallis entropy measure (TE), as well as the Havrda and Charvat entropy measure (HCE), all of which are formally derived in Sections 3.4.1–3.4.3, respectively.

3.4.1. Rényi Entropy

If $X \sim$ *new-G* $(x;\Theta)$ with scale $(\alpha > 0)$ and vector space (Θ) the $RE|_{x;\Theta}$ of the new-PFD is defined as follows:

$$RE|_x = \frac{1}{1-\Omega} log \int_0^M [f|_{x;\Theta}]^{\Omega} dx. \tag{19}$$

We get the simplified form of $[f|_{x;\Theta}]^{\Omega}$ by solving (6) in terms of Ω,

$$[f|_{x;\Theta}]^{\Omega} = \sum_{l_1,l_2,l_3=0}^{\infty}\left[\binom{\Omega}{l_1}\frac{[l_1]^{l_2}[log(1+\alpha)]^{\Omega-l_1+l_3}}{l_2!l_3!}[log(\alpha)]^{l_1+l_2}(-1)^{l_1}2^{l_1}(\Omega-l_1)^{l_3}\frac{\theta^{\Omega}}{M^{\Omega\theta+\theta(l_1+2l_2+l_3)}}x^{\Omega(\theta-1)+\theta(l_1+2l_2+l_3)}\right]\Bigg|_{\alpha,\Omega>0,\Omega\neq1,x\in\Re}. \tag{20}$$

Hence, the final form of $RE|_{x;\Theta}$ is obtained when (20) is placed into (19)

$$RE|_x = \frac{1}{1-\Omega} log \sum_{l_1,l_2,l_3=0}^{\infty}\left[\binom{\Omega}{l_1}\frac{[l_1]^{l_2}[log(1+\alpha)]^{\Omega-l_1+l_3}}{l_2!l_3!}[log(\alpha)]^{l_1+l_2}(-1)^{l_1}2^{l_1}(\Omega-l_1)^{l_3}\frac{\theta^{\Omega}M^{1-\Omega}}{[\Omega(\theta-1)+\theta(l_1+2l_2+l_3)+1]}\right]\Bigg|_{\alpha,\Omega,\theta>0,\Omega\neq1,x\in\Re}.$$

3.4.2. Tsallis Entropy

If $X \sim$ *new-PFD* $(x;\Theta)$ with scale $(\alpha > 0)$ and vector space (Θ), the $TE|_{x;\Theta}$ of the new-PFD is defined as follows:

$$TE|_x = \frac{1}{1-\Omega}\int_{-\infty}^{+\infty}[f|_{x;\Theta}]^{\Omega}dx - 1. \tag{21}$$

Hence, we get the final form of $TE|_{x;\Theta}$ when (20) is placed into (21)

$$TE|_x = \frac{1}{1-\Omega}\sum_{l_1,l_2,l_3=0}^{\infty}\left[\binom{\Omega}{l_1}\frac{[l_1]^{l_2}[log(1+\alpha)]^{\Omega-l_1+l_3}}{l_2!l_3!}[log(\alpha)]^{l_1+l_2}(-1)^{l_1}2^{l_1}(\Omega-l_1)^{l_3}\frac{\theta^{\Omega}M^{1-\Omega}}{[\Omega(\theta-1)+\theta(l_1+2l_2+l_3)+1]}\right]-1\Bigg|_{\alpha,\Omega,\theta>0,\Omega\neq1,x\in\Re}.$$

3.4.3. Havrda and Charvat Entropy

If $X \sim$ *new-G* $(x;\Theta)$ with scale $(\alpha > 0)$ and vector space (Θ), the $HCE|_{x;\Theta}$ of the new-G is defined as follows:

$$HCE|_x = A\int_{-\infty}^{+\infty} [f|_{x;\Theta}]^{\Omega} dx - 1. \tag{22}$$

Hence, we get the final form of $HCE|_{x;\Theta}$ when (20) is placed into (22)

$$HCE|_x = A\sum_{l_1,l_2,l_3=0}^{\infty} \left[\begin{array}{c} \binom{\Omega}{l_1} \frac{[l_1]^{l_2}[log(1+\alpha)]^{\Omega-l_1+l_3}}{l_2! l_3!} \\ [log(\alpha)]^{l_1+l_2}(-1)^{l_1} 2^{l_1} \\ (\Omega - l_1)^{l_3} \frac{\theta^{\Omega} M^{1-\Omega}}{[\Omega(\theta-1)+\theta(l_1+2l_2+l_3)+1]} \end{array} \right] - 1 \Bigg|_{\alpha,\Omega,\theta>0,\Omega\neq 1,x\in\Re},$$

where $A = \frac{1}{2^{1-\Omega}-1}$. It should be noted that any software, such as R or Mathematica, can easily perform its numerical analysis.

3.5. Order Statistics (OS)

Suppose $X|_1, X|_2, X|_3, \ldots, X|_n$ be (iid) independent, identically distributed, random variables *(RVs)* from the new-G family of distributions. The pdf and cdf of the *j*-th OS $X|_{j:n}$ are, respectively, presented by

$$f_{j:n}\big|_x = \frac{1}{B(a,b)}[F|_x]^{j-1}[f|_x][1 - F|_x]^{n-j}.$$

$$f_{j:n}\big|_x = \left[\begin{array}{c} \frac{1}{B(a,b)} \left[(1+\alpha)^{[\frac{x}{M}]^{\theta}} - \alpha^{[\frac{x}{M}]^{2\theta}} \right]^{j-1} \times \\ \left[\frac{\theta}{M}\right] \left[\frac{x}{M}\right]^{\theta-1} \left[\begin{array}{c} (1+\alpha)^{[\frac{x}{M}]^{\theta}} log(1+\alpha) - \\ 2\left[\frac{x}{M}\right]^{\theta} \alpha^{[\frac{x}{M}]^{2\theta}} log\alpha \end{array} \right] \times \\ \left[1 - (1+\alpha)^{[\frac{x}{M}]^{\theta}} + \alpha^{[\frac{x}{M}]^{2\theta}} \right]^{n-j} \end{array} \right],$$

and

$$F_{j:n}\big|_x = \sum_{r=i}^{n} \binom{n}{r} [F_x]^r [1 - F|_x]^{n-r},$$

$$F_{j:n}\big|_x = \sum_{r=i}^{n} \binom{n}{r} \left[(1+\alpha)^{[\frac{x}{M}]^{\theta}} - \alpha^{[\frac{x}{M}]^{2\theta}} \right]^r \left[1 - (1+\alpha)^{[\frac{x}{M}]^{\theta}} + \alpha^{[\frac{x}{M}]^{2\theta}} \right]^{n-r},$$

where $B(a,b) = B(j, n-j+1)$. It is worth noting that the minimum and maximum OS pdf are obtained by substituting in $n = 0$ and $n = 1$, respectively.

4. Inference

This section briefly illustrates the performance of our estimation methods as presented in (Sections 4.1–4.6). For this, cdf (5) is considered our baseline model.

4.1. Maximum Likelihood Estimation Method (MLE)

Let $X_j \sim$ *new-PFD* $(x_j;\alpha,\theta)$ with scale $(\alpha > 0)$ and shape (θ) parameters, then the log-likelihood $l|_x$ from a random sample $x_1, x_2, x_3, \ldots, x_n$ of size n from (6), is given by

$$l|_x = nlog\theta - n\theta logM + (\theta - 1)\sum_{j=1}^{n} logx_j + \sum_{j=1}^{n} log[p|_1 - p|_2] \Big|_{\alpha,\theta>0,M\geq x_j}.$$

The partial derivative of $l|_{\Theta}$ is provided in the following form for both α and θ, respectively:

$$\frac{\partial l|_x}{\partial \alpha} = \sum_{j=1}^{n} \frac{1}{p|_1 - p|_2} \begin{bmatrix} (1+\alpha)^{\left[\frac{x_j}{M}\right]^{\theta}-1} \left\{ \left[\frac{x_j}{M}\right]^{\theta} log(1+\alpha) + 1 \right\} - \\ 2\alpha^{\left[\frac{x_j}{M}\right]^{2\theta}-1} \left[\frac{x_j}{M}\right]^{\theta} \left\{ \left[\frac{x_j}{M}\right]^{2\theta} log\alpha + 1 \right\} \end{bmatrix},$$

$$\frac{\partial l|_x}{\partial \theta} = n\left[\frac{1}{\theta} - logM\right] + \sum_{j=1}^{n} logx_j + \sum_{j=1}^{n} \frac{1}{p|_1 - p|_2} \left[log\left[\frac{x_j}{M}\right] \begin{bmatrix} (1+\alpha)^{\left[\frac{x_j}{M}\right]^{\theta}} \{log(1+\alpha)\}^2 - \\ 4\alpha^{\left[\frac{x_j}{M}\right]^{2\theta}} \{log\alpha\}^2 \left[\frac{x_j}{M}\right]^{\theta} - \\ 2\alpha^{\left[\frac{x_j}{M}\right]^{2\theta}} log\alpha \left[\frac{x_j}{M}\right]^{\theta} \end{bmatrix} \right],$$

where $p|_1 = (1+\alpha)^{\left[\frac{x_j}{M}\right]^{\theta}} log(1+\alpha)$ and $p|_2 = 2\left[\frac{x_j}{M}\right]^{\theta} \alpha^{\left[\frac{x_j}{M}\right]^{2\theta}} log\alpha$.

4.2. Anderson–Darling Estimation Method (ADE-M)

Let $X_j \sim$ *new-PFD* $(x_j; \alpha, \theta)$ with scale $(\alpha > 0)$ and shape (θ) parameter, then the estimators of our proposed family is obtained by the Anderson–Darling estimation by minimizing the following expression:

$$ADE - M = -n - \frac{1}{n}\sum_{j=1}^{n}(2j-1)\Big(log F_x|_{j:n} + log\left(1 - F_x|_{j:n}\right)\Big).$$

4.3. Cram'er–Von Mises Estimation Method (CVME-M)

Let $X_j \sim$ *new-PFD* $(x_j; \alpha, \theta)$ with scale $(\alpha > 0)$ and shape (θ) parameter, then the estimators of our proposed family is obtained by the Cram´er–von Mises estimation by minimizing the following expression:

$$CVME - M = \frac{1}{12n} + \sum_{j=1}^{n}\left(F_x|_{j:n} - \frac{2j-1}{2n}\right)^2.$$

4.4. Least Squares Estimation Method (LSE-M)

Let $X_j \sim$ *new-PFD* $(x_j; \alpha, \theta)$ with scale $(\alpha > 0)$ and shape (θ) parameter, then the estimators of our proposed family is obtained by the least-squares estimation by minimizing the following expression:

$$LSE - M = \sum_{j=1}^{n}\left(F_x|_{j:n} - \frac{j}{n+1}\right)^2.$$

4.5. Weighted Least-Squares Estimation Method (WLSE-M)

Let $X_j \sim$ *new-PFD* $(x_j; \alpha, \theta)$ with scale $(\alpha > 0)$ and shape (θ) parameter, then the estimators of our proposed family is obtained by the weighted least-squares estimation by minimizing the following expression:

$$WLSE - M = \frac{(n+1)^2(n+2)}{j(n-j+1)}\sum_{j=1}^{n}\left(F_x|_{j:n} - \frac{j}{n+1}\right)^2.$$

4.6. Maximum Product of Spacings Estimation Method (MPSE-M)

Let $X_j \sim$ *new-PFD* $(x_j; \alpha, \theta)$ with scale $(\alpha > 0)$ and shape (θ) parameter, then the estimators of our proposed family is obtained by the maximum product of the spacings estimation by maximizing the following expression:

$$MPSE - M = \frac{1}{(n+1)} \sum_{j=1}^{n+1} (log F_x|_j - F_x|_{j-1})^2.$$

5. Simulation Study

The simulation work is one of the most vital components of any kind of paper. The purpose of this part is to investigate the performance of the estimation techniques that have been presented in order to estimate the parameters of the new-PFD utilizing the results of thorough simulations. We used different sample sizes along with different values of parameters, as we can see in Tables 2–5. We observed that the average absolute biases ($|BIAS|$), mean square errors (MSEs), and mean relative errors (MREs) decreased as the sample size increased for all parameter values. Now, we can conclude that all estimates have the consistency property and all estimation methods performed well. This simulation study is based on the following algorithm:

1. We set the beginning values for the parameters of our suggested model.
2. From our suggested model, we have produced random data sets using the inverse of cdf.
3. Use several estimate techniques to find estimators for our proposed model.
4. Calculate the bias, MSE, and MRE for each estimator using each estimating technique.
5. Repeat steps 1 through 4, 500 times.

$$|BIAS| = \frac{1}{500} \sum_{k=1}^{500} |\hat{\Lambda} - \Lambda|,$$

$$MSEs = \frac{1}{500} \sum_{k=1}^{500} (\hat{\Lambda} - \Lambda)^2,$$

$$MREs = \frac{1}{500} \sum_{k=1}^{500} |\hat{\Lambda} - \Lambda| / \Lambda.$$

Table 2. The simulated BIAS, MSE, and MRE values for (α = 0.5, θ = 1.5).

n	Est.	Par.	MLE-M	ADE-M	CVME-M	MPSE-M	LSE-M	WLSE-M
20	BIAS	$\hat{\alpha}$	0.3769	0.3296	0.3288	0.3120	0.3697	0.3932
		$\hat{\theta}$	0.3723	0.3683	0.3915	0.3293	0.3241	0.4479
	MSE	$\hat{\alpha}$	0.2035	0.1671	0.1498	0.1352	0.1689	0.1946
		$\hat{\theta}$	0.2903	0.2374	0.3020	0.1866	0.1949	0.4083
	MRE	$\hat{\alpha}$	0.7538	0.6593	0.6576	0.6240	0.7394	0.7864
		$\hat{\theta}$	0.2482	0.2455	0.2610	0.2196	0.2161	0.2986
40	BIAS	$\hat{\alpha}$	0.3226	0.3177	0.2933	0.2955	0.3218	0.3115
		$\hat{\theta}$	0.2652	0.2654	0.2669	0.2128	0.2719	0.2403
	MSE	$\hat{\alpha}$	0.1698	0.1469	0.1170	0.1294	0.1392	0.1394
		$\hat{\theta}$	0.1128	0.1173	0.1192	0.0843	0.1251	0.1109
	MRE	$\hat{\alpha}$	0.6451	0.6354	0.5865	0.5910	0.6435	0.6229
		$\hat{\theta}$	0.1768	0.1770	0.1780	0.1419	0.1813	0.1602

Table 2. *Cont.*

n	Est.	Par.	MLE-M	ADE-M	CVME-M	MPSE-M	LSE-M	WLSE-M
80	BIAS	$\hat{\alpha}$	0.2865	0.2372	0.2258	0.2450	0.2577	0.2499
		$\hat{\theta}$	0.1836	0.1790	0.1891	0.1689	0.1741	0.1767
	MSE	$\hat{\alpha}$	0.1457	0.0925	0.0828	0.0998	0.1098	0.1059
		$\hat{\theta}$	0.0632	0.0521	0.0550	0.0538	0.0547	0.0535
	MRE	$\hat{\alpha}$	0.5730	0.4744	0.4516	0.4901	0.5154	0.4999
		$\hat{\theta}$	0.1224	0.1193	0.1261	0.1126	0.1161	0.1178
100	BIAS	$\hat{\alpha}$	0.2538	0.2231	0.2604	0.2140	0.2631	0.2727
		$\hat{\theta}$	0.1768	0.1661	0.1741	0.1501	0.1812	0.1577
	MSE	$\hat{\alpha}$	0.1142	0.0816	0.1062	0.0832	0.1109	0.1151
		$\hat{\theta}$	0.0556	0.0482	0.0519	0.0413	0.0528	0.0449
	MRE	$\hat{\alpha}$	0.5076	0.4462	0.5207	0.4279	0.5262	0.5455
		$\hat{\theta}$	0.1178	0.1107	0.1161	0.1001	0.1208	0.1051
150	BIAS	$\hat{\alpha}$	0.2357	0.2039	0.2321	0.2295	0.2092	0.2634
		$\hat{\theta}$	0.1523	0.1357	0.1600	0.1158	0.1319	0.1414
	MSE	$\hat{\alpha}$	0.1210	0.0779	0.0974	0.1005	0.0906	0.1184
		$\hat{\theta}$	0.0479	0.0300	0.0528	0.0248	0.0431	0.0302
	MRE	$\hat{\alpha}$	0.4713	0.4078	0.4641	0.4590	0.4183	0.5269
		$\hat{\theta}$	0.1015	0.0905	0.1067	0.0772	0.0879	0.0942
200	BIAS	$\hat{\alpha}$	0.2177	0.1687	0.2269	0.1551	0.2126	0.2236
		$\hat{\theta}$	0.1270	0.1073	0.1115	0.0926	0.1097	0.1222
	MSE	$\hat{\alpha}$	0.1030	0.0600	0.0978	0.0514	0.0872	0.0980
		$\hat{\theta}$	0.0273	0.0193	0.0217	0.0159	0.0200	0.0248
	MRE	$\hat{\alpha}$	0.4353	0.3375	0.4538	0.3101	0.4251	0.4472
		$\hat{\theta}$	0.0847	0.0715	0.0743	0.0617	0.0731	0.0815

Table 3. The simulated BIAS, MSE, and MRE values for (α = 0.75, θ = 0.5).

n	Est.	Par.	MLE-M	ADE-M	CVME-M	MPSE-M	LSE-M	WLSE-M
20	BIAS	$\hat{\alpha}$	0.4524	0.3208	0.3965	0.2681	0.3433	0.3426
		$\hat{\theta}$	0.1327	0.1265	0.1600	0.1030	0.1352	0.1349
	MSE	$\hat{\alpha}$	0.2718	0.1350	0.1910	0.1034	0.1455	0.1650
		$\hat{\theta}$	0.0383	0.0277	0.0426	0.0238	0.0330	0.0374
	MRE	$\hat{\alpha}$	0.6032	0.4278	0.5287	0.3575	0.4577	0.4568
		$\hat{\theta}$	0.2655	0.2529	0.3199	0.2060	0.2705	0.2698
40	BIAS	$\hat{\alpha}$	0.3773	0.2905	0.3601	0.2529	0.3060	0.3293
		$\hat{\theta}$	0.0824	0.0786	0.1078	0.0616	0.0942	0.0795
	MSE	$\hat{\alpha}$	0.2131	0.1143	0.1548	0.1018	0.1112	0.1374
		$\hat{\theta}$	0.0141	0.0115	0.0183	0.0083	0.0152	0.0106
	MRE	$\hat{\alpha}$	0.5031	0.3873	0.4802	0.3372	0.4080	0.4390
		$\hat{\theta}$	0.1649	0.1572	0.2157	0.1231	0.1884	0.1590

Table 3. *Cont.*

n	Est.	Par.	MLE-M	ADE-M	CVME-M	MPSE-M	LSE-M	WLSE-M
80	BIAS	$\hat{\alpha}$	0.2763	0.2139	0.3093	0.2312	0.2794	0.2613
		$\hat{\theta}$	0.0497	0.0542	0.0661	0.0419	0.0647	0.0602
	MSE	$\hat{\alpha}$	0.1272	0.0754	0.1120	0.0938	0.0978	0.0858
		$\hat{\theta}$	0.0053	0.0061	0.0081	0.0035	0.0078	0.0062
	MRE	$\hat{\alpha}$	0.3684	0.2852	0.4125	0.3083	0.3725	0.3484
		$\hat{\theta}$	0.0993	0.1084	0.1321	0.0838	0.1293	0.1203
100	BIAS	$\hat{\alpha}$	0.2598	0.1988	0.2691	0.1739	0.2452	0.2783
		$\hat{\theta}$	0.0428	0.0445	0.0514	0.0311	0.0547	0.0606
	MSE	$\hat{\alpha}$	0.1216	0.0647	0.0946	0.0633	0.0823	0.0992
		$\hat{\theta}$	0.0045	0.0043	0.0045	0.0024	0.0047	0.0065
	MRE	$\hat{\alpha}$	0.3464	0.2650	0.3589	0.2318	0.3270	0.3711
		$\hat{\theta}$	0.0856	0.0890	0.1028	0.0623	0.1094	0.1212
150	BIAS	$\hat{\alpha}$	0.2659	0.1839	0.2481	0.1731	0.2767	0.2420
		$\hat{\theta}$	0.0446	0.0318	0.0465	0.0334	0.0446	0.0439
	MSE	$\hat{\alpha}$	0.1286	0.0632	0.0792	0.0642	0.0901	0.0779
		$\hat{\theta}$	0.0046	0.0022	0.0035	0.0027	0.0033	0.0031
	MRE	$\hat{\alpha}$	0.3546	0.2453	0.3307	0.2308	0.3690	0.3227
		$\hat{\theta}$	0.0893	0.0636	0.0930	0.0668	0.0891	0.0879
200	BIAS	$\hat{\alpha}$	0.2047	0.1354	0.2469	0.1375	0.2556	0.2536
		$\hat{\theta}$	0.0317	0.0268	0.0484	0.0223	0.0428	0.0427
	MSE	$\hat{\alpha}$	0.0950	0.0386	0.0761	0.0481	0.0814	0.0781
		$\hat{\theta}$	0.0030	0.0018	0.0037	0.0013	0.0029	0.0032
	MRE	$\hat{\alpha}$	0.2730	0.1805	0.3292	0.1833	0.3408	0.3381
		$\hat{\theta}$	0.0633	0.0536	0.0967	0.0446	0.0856	0.0854

Table 4. The simulated BIAS, MSE, and MRE values for (α = 2.5, θ = 0.75).

n	Est.	Par.	MLE-M	ADE-M	CVME-M	MPSE-M	LSE-M	WLSE-M
20	BIAS	$\hat{\alpha}$	1.1442	0.2833	0.3719	0.3823	0.4131	0.3160
		$\hat{\theta}$	0.1602	0.1293	0.1434	0.1475	0.1504	0.1414
	MSE	$\hat{\alpha}$	1.6432	0.1557	0.2312	0.2903	0.2905	0.1607
		$\hat{\theta}$	0.0408	0.0307	0.0316	0.0331	0.0361	0.0305
	MRE	$\hat{\alpha}$	0.4577	0.1133	0.1488	0.1529	0.1653	0.1264
		$\hat{\theta}$	0.2136	0.1724	0.1912	0.1967	0.2005	0.1885
40	BIAS	$\hat{\alpha}$	0.8187	0.1869	0.3060	0.2338	0.3459	0.2289
		$\hat{\theta}$	0.1534	0.0950	0.1106	0.0853	0.1104	0.1052
	MSE	$\hat{\alpha}$	1.1100	0.0648	0.1467	0.1348	0.2198	0.0965
		$\hat{\theta}$	0.0428	0.0135	0.0195	0.0115	0.0204	0.0181
	MRE	$\hat{\alpha}$	0.3275	0.0747	0.1224	0.0935	0.1384	0.0916
		$\hat{\theta}$	0.2045	0.1267	0.1474	0.1138	0.1473	0.1402

Table 4. *Cont.*

n	Est.	Par.	MLE-M	ADE-M	CVME-M	MPSE-M	LSE-M	WLSE-M
80	BIAS	$\hat{\alpha}$	0.5424	0.1206	0.1838	0.1014	0.1968	0.1544
		$\hat{\theta}$	0.1142	0.0673	0.0815	0.0586	0.0770	0.0759
	MSE	$\hat{\alpha}$	0.6064	0.0286	0.0564	0.0168	0.0653	0.0417
		$\hat{\theta}$	0.0250	0.0072	0.0104	0.0057	0.0090	0.0082
	MRE	$\hat{\alpha}$	0.2170	0.0483	0.0735	0.0406	0.0787	0.0618
		$\hat{\theta}$	0.1523	0.0897	0.1087	0.0781	0.1027	0.1012
100	BIAS	$\hat{\alpha}$	0.5402	0.0992	0.1572	0.0818	0.1865	0.1131
		$\hat{\theta}$	0.1370	0.0632	0.0556	0.0457	0.0674	0.0526
	MSE	$\hat{\alpha}$	0.5514	0.0184	0.0420	0.0111	0.0506	0.0200
		$\hat{\theta}$	0.0362	0.0064	0.0051	0.0037	0.0075	0.0046
	MRE	$\hat{\alpha}$	0.2161	0.0397	0.0629	0.0327	0.0746	0.0452
		$\hat{\theta}$	0.1826	0.0843	0.0741	0.0609	0.0898	0.0702
150	BIAS	$\hat{\alpha}$	0.3914	0.0701	0.1261	0.0587	0.1387	0.0879
		$\hat{\theta}$	0.0915	0.0393	0.0524	0.0397	0.0517	0.0486
	MSE	$\hat{\alpha}$	0.3582	0.0099	0.0252	0.0066	0.0318	0.0118
		$\hat{\theta}$	0.0172	0.0025	0.0043	0.0026	0.0040	0.0038
	MRE	$\hat{\alpha}$	0.1566	0.0281	0.0504	0.0235	0.0555	0.0352
		$\hat{\theta}$	0.1221	0.0523	0.0699	0.0530	0.0690	0.0648
200	BIAS	$\hat{\alpha}$	0.2187	0.0536	0.1108	0.0354	0.1192	0.0755
		$\hat{\theta}$	0.0579	0.0378	0.0487	0.0299	0.0453	0.0406
	MSE	$\hat{\alpha}$	0.0880	0.0064	0.0195	0.0022	0.0225	0.0082
		$\hat{\theta}$	0.0068	0.0025	0.0035	0.0017	0.0031	0.0027
	MRE	$\hat{\alpha}$	0.0875	0.0215	0.0443	0.0142	0.0477	0.0302
		$\hat{\theta}$	0.0772	0.0504	0.0649	0.0398	0.0604	0.0542

Table 5. The simulated BIAS, MSE, and MRE values for (α = 1.5, θ = 2.5).

n	Est.	Par.	MLE-M	ADE-M	CVME-M	MPSE-M	LSE-M	WLSE-M
20	BIAS	$\hat{\alpha}$	0.6551	0.5539	0.5667	0.5194	0.5117	0.5046
		$\hat{\theta}$	0.5853	0.5147	0.5672	0.5333	0.5370	0.5565
	MSE	$\hat{\alpha}$	0.8185	0.4264	0.4388	0.3312	0.3496	0.3353
		$\hat{\theta}$	0.5296	0.4334	0.5226	0.3938	0.4555	0.4805
	MRE	$\hat{\alpha}$	0.4367	0.3693	0.3778	0.3463	0.3411	0.3364
		$\hat{\theta}$	0.2341	0.2059	0.2269	0.2133	0.2148	0.2226
40	BIAS	$\hat{\alpha}$	0.4699	0.4312	0.4480	0.4797	0.4561	0.4303
		$\hat{\theta}$	0.4674	0.4015	0.4695	0.4247	0.3905	0.4035
	MSE	$\hat{\alpha}$	0.2956	0.2428	0.2840	0.3135	0.2724	0.2252
		$\hat{\theta}$	0.3515	0.2245	0.3717	0.2447	0.2339	0.2738
	MRE	$\hat{\alpha}$	0.3133	0.2875	0.2987	0.3198	0.3041	0.2869
		$\hat{\theta}$	0.1870	0.1606	0.1878	0.1699	0.1562	0.1614

Table 5. *Cont.*

n	Est.	Par.	MLE-M	ADE-M	CVME-M	MPSE-M	LSE-M	WLSE-M
80	BIAS	$\hat{\alpha}$	0.3615	0.3707	0.3991	0.3688	0.3920	0.3369
		$\hat{\theta}$	0.3561	0.2647	0.3746	0.3453	0.3465	0.2991
	MSE	$\hat{\alpha}$	0.1906	0.1830	0.2170	0.1995	0.2006	0.1527
		$\hat{\theta}$	0.1944	0.1216	0.2243	0.1818	0.1802	0.1374
	MRE	$\hat{\alpha}$	0.2410	0.2471	0.2661	0.2459	0.2613	0.2246
		$\hat{\theta}$	0.1424	0.1059	0.1498	0.1381	0.1386	0.1197
100	BIAS	$\hat{\alpha}$	0.3808	0.3453	0.3706	0.4104	0.3278	0.3254
		$\hat{\theta}$	0.3515	0.2927	0.3085	0.3352	0.2728	0.2765
	MSE	$\hat{\alpha}$	0.1986	0.1607	0.1639	0.2329	0.1525	0.1499
		$\hat{\theta}$	0.1995	0.1271	0.1579	0.1677	0.1200	0.1195
	MRE	$\hat{\alpha}$	0.2539	0.2302	0.2470	0.2736	0.2185	0.2170
		$\hat{\theta}$	0.1406	0.1171	0.1234	0.1341	0.1091	0.1106
150	BIAS	$\hat{\alpha}$	0.2997	0.2534	0.3034	0.3213	0.3070	0.3110
		$\hat{\theta}$	0.2417	0.2349	0.2779	0.2508	0.2770	0.2720
	MSE	$\hat{\alpha}$	0.1447	0.1010	0.1283	0.1701	0.1295	0.1376
		$\hat{\theta}$	0.0890	0.0881	0.1206	0.0988	0.1082	0.1020
	MRE	$\hat{\alpha}$	0.1998	0.1689	0.2023	0.2142	0.2047	0.2073
		$\hat{\theta}$	0.0967	0.0940	0.1112	0.1003	0.1108	0.1088
200	BIAS	$\hat{\alpha}$	0.2640	0.2652	0.3074	0.3507	0.2594	0.2394
		$\hat{\theta}$	0.2121	0.2225	0.2266	0.2427	0.2349	0.2063
	MSE	$\hat{\alpha}$	0.1234	0.1032	0.1193	0.1943	0.0987	0.0902
		$\hat{\theta}$	0.0762	0.0796	0.0746	0.0966	0.0821	0.0654
	MRE	$\hat{\alpha}$	0.1760	0.1768	0.2050	0.2338	0.1729	0.1596
		$\hat{\theta}$	0.0848	0.0890	0.0906	0.0971	0.0940	0.0825

6. Analysis of COVID-19 Data

The new-PFD and well-known competitors were statistically analysed using the COVID-19 data.

The first data set describes 76-day COVID-19 mortality rates in the United Kingdom (15 April to 30 June 2020). The second data set describes the daily death toll in Europe as specified in the COVID-19 data (1 March to 30 March). The third data set describes the daily death toll in China as specified in the COVID-19 data (23 January to 28 January). The fourth data set describes the mortality rates from COVID-19 data for the United Kingdom for 24 days (15 October to 7 November 2020). The fifth data set describes the mortality rates from COVID-19 data for Nepal (23 January 2020 to 24 December 2020). The sixth data set describes the mortality rates from COVID-19 data for the Netherlands for 30 days (31 March 2020 to 30 April 2020). The seventh data set describes the mortality rates from COVID-19 data for Italy for a period of 59 days (27 February 2020 to 27 April 2020).

Tables 6–12 present estimates and fitted measures for all COVID-19 mortality datasets. The definition of a better model fit is quite straightforward: when the model is used, the model is considered to be a better fit if the minimum results (see Tables 6–12) of Akaike information criterion (AIC), Cramer-von Mises (CVM), Anderson Darling (AD), sum of

square (SS), and Kolmogorov–Smirnov (KS) (with a high *p*-value of KS) are met. The acknowledged statistical measures are defined as follows:

$$\text{AIC} = 2k - 2\log(LL),$$

$$\text{CVM} = \frac{1}{12n} + \sum_{j=1}^{n}\left(F_x|_{j:n} - \frac{2j-1}{2n}\right)^2,$$

$$\text{AD} = -n - \frac{1}{n}\sum_{j=1}^{n}(2j-1)\left(log\,F_x|_{j:n} + log\,(1 - F_x|_{j:n})\right),$$

$$\text{KS} = \sup_x\left|F_x|_{j:n} - F|_x\right|$$

$$\text{SS} = \sum_{j=1}^{n}\left(F_x|_{j:n} - \frac{j-0.375}{n+0.250}\right)^2,$$

where k is the number of parameters being used and LL is the log-likelihood of the models being used.

Table 6. Estimates and Fitted Measures for United Kingdom Mortality Rate.

Model	Estimates			Fitted Measures					
	$\hat{\alpha}$	$\hat{\theta}$	$\hat{\gamma}$	AIC	CVM	AD	KS	*p*-Value	SS
New-PFD	0.0314	0.4012	-	283.6512	0.1934	1.2679	0.0777	0.7488	0.1147
Tr-PF	0.7647	-	1.5949	291.6001	0.3140	1.9964	0.1329	0.1367	0.3548
Kum-PF	1.1071	0.4754	1.3700	302.9045	0.4286	2.6819	0.1582	0.0446	0.5521
OGE-PF	6.4256	0.0690	2.0309	309.0742	0.3635	2.3533	0.1959	0.0058	0.9499
PF-I	0.4375	-	-	302.9309	0.4179	2.6213	0.1976	0.0053	0.9699
NG-PF	0.6775	0.0727	5.8366	305.8946	0.3440	2.1834	0.0777	0.0038	1.0395
Gen-PF	2.2790	-	-	332.1345	0.3500	2.1641	0.3180	0.0000	3.0369

Table 7. Estimates and Fitted Measures for Europe Mortality Rate.

Model	Estimates			Fitted Measures					
	$\hat{\alpha}$	$\hat{\theta}$	$\hat{\gamma}$	AIC	CVM	AD	KS	*p*-Value	SS
New-PFD	0.1921	0.3262	-	470.1407	0.1433	0.9490	0.1232	0.6889	0.0760
ZTP-PF	2.8368	0.7329	-	476.5421	-	-	0.1728	0.2790	0.1924
Kum-PF	1.2485	0.2696	0.6369	467.5365	0.1976	1.2621	0.1797	0.2393	0.2962
OGE-PF	4.7180	0.0646	0.0047	475.6623	0.1195	0.8823	0.2213	0.0818	0.4595
Gen-PF	1.0351	-	-	494.4784	0.1204	0.7690	0.3991	0.0001	1.8877

Table 8. Estimates and Fitted Measures for China Mortality Rate.

Model	Estimates			Fitted Measures					
	$\hat{\alpha}$	$\hat{\theta}$	$\hat{\gamma}$	AIC	CVM	AD	KS	*p*-Value	SS
New-PFD	0.1044	0.4908	-	642.4877	0.1217	0.8393	0.0814	0.7740	0.0924
Tr-PF	0.5604	-	1.7920	643.7063	0.1588	1.0521	0.1032	0.4836	0.1446

Table 8. *Cont.*

Model	Estimates			Fitted Measures					
	$\hat{\alpha}$	$\hat{\theta}$	$\hat{\gamma}$	AIC	CVM	AD	KS	*p*-Value	SS
NG-PF	1.1644	17.2847	0.0531	648.6244	0.1868	1.2314	0.0814	0.2892	0.1946
Kum-PF	0.3894	1.6505	1.0472	650.1455	0.2125	1.3840	0.1464	0.1182	0.2983
PF-I	0.6247	-	-	646.2304	0.2118	1.3797	0.1521	0.0945	0.3314

Table 9. Estimates and Fitted Measures for United Kingdom Mortality Rate.

Model	Estimates			Fitted Measures					
	$\hat{\alpha}$	$\hat{\theta}$	$\hat{\gamma}$	AIC	CVM	AD	KS	*p*-Value	SS
New-PFD	0.0287	1.3984	-	−41.7665	0.0255	0.2089	0.0835	0.9910	0.0199
NG-PF	1.5971	18.5499	0.2342	−38.5436	0.0361	0.3030	0.0835	0.9651	0.0265
Kum-PF	0.9756	2.1057	1.7528	−36.7425	0.0532	0.4306	0.1276	0.7836	0.0555
Tr-PF	0.8341	-	1.0780	−39.9779	0.0382	0.3138	0.1277	0.7826	0.0522
PF-I	1.4845	-	-	−37.2526	0.0498	0.4067	0.2310	0.1311	0.2499

Table 10. Estimates and Fitted Measures for Nepal Mortality Rate.

Model	Estimates			Fitted Measures					
	$\hat{\alpha}$	$\hat{\theta}$	$\hat{\gamma}$	AIC	CVM	AD	KS	*p*-Value	SS
New-PFD	0.0205	0.8481	-	993.5991	0.0471	0.4678	0.0519	0.8044	0.0531
W-PF	4.2216	8.4898	0.2024	996.1838	0.0597	0.5134	0.0548	0.7468	0.0594
ZTP-PF	4.3987	1.7816	-	998.4550	0.1012	0.8065	0.0679	0.4803	0.1028
MOE-PF	0.1416	1.9682	-	994.8340	0.0874	0.7155	0.0681	0.4774	0.0815
Gen-PF	1.7756	-	-	979.7377	0.5117	3.7593	0.0716	0.4132	0.1176
Kum-PF	0.4168	3.0564	1.9823	1012.3107	0.1206	0.9920	0.0790	0.2948	0.1706
Tr-PF	0.9380	-	1.2519	1002.0116	0.0784	0.6836	0.0819	0.2563	0.1993
OGE-PF	7.6256	0.1239	2.8673	1035.8485	0.2114	1.5872	0.1621	0.0006	1.0577
PF-I	0.8615	-	-	1039.2363	0.1050	0.8905	0.1992	0.0000	1.6514

Table 11. Estimates and Fitted Measures for Netherlands Mortality Rate.

Model	Estimates			Fitted Measures					
	$\hat{\alpha}$	$\hat{\theta}$	$\hat{\gamma}$	AIC	CVM	AD	KS	*p*-Value	SS
New-PFD	0.0253	0.8957	-	156.8105	0.1062	0.6493	0.1070	0.8467	0.0522
PF-Poi	−3.5098	1.7625	-	156.8312	0.1076	0.6575	0.1093	0.8283	0.0549
Tr-PF	0.8025	-	1.3066	160.1585	0.1701	1.0188	0.1617	0.3725	0.1589
NG-PF	1.3880			164.1245	0.1819	1.1150	0.1070	0.3563	0.1619
Kum-PF	0.4400	2.4843	1.2740	167.1066	0.2316	1.4057	0.2097	0.1232	0.2811
OGE-PF	9.8176	0.1003	2.8782	168.6015	0.1665	0.9571	0.2378	0.0562	0.3771

Table 12. Estimates and Fitted Measures for Italy Mortality Rate.

Model	Estimates			Fitted Measures					
	$\hat{\alpha}$	$\hat{\theta}$	$\hat{\gamma}$	AIC	CVM	AD	KS	p-Value	SS
New-PFD	0.0442	0.8961	-	335.7237	0.0979	0.7027	0.1128	0.4103	0.1011
Tr-PF	0.8247	-	1.4090	338.2626	0.1176	0.8627	0.1162	0.3742	0.1269
Kum-PF	0.5666	2.2183	1.4513	345.9732	0.1472	1.1037	0.1172	0.3639	0.1927
NG-PF	1.4465	27.0812	0.0996	341.4392	0.1092	0.8408	0.1128	0.3496	0.1173
OGE-PF	8.7252	0.1239	2.8958	349.0370	0.1462	1.0418	0.1414	0.1718	0.3554
ZTP-PF	3.8076	1.9272	-	339.4020	0.1315	0.7659	0.1450	0.1514	0.1789
PF-I	1.0090	-	-	346.1583	0.1420	1.0706	0.1694	0.0598	0.4853

When compared to well-known models such as Tr-PF by Haq et al. [5], Kum-PF by Moniem [26], OGE-PF by Tahir et al. [27], PF-I and NG-PF by Hassan and Nassr [28], ZTP-PF by Okorie et al. [29], and MOE-PF by Okorie et al. [30], the proposed new-PFD better fits the COVID-19 mortality rates in the United Kingdom, Europe, China, the United Kingdom, Nepal, the Netherlands, and Italy. All these data sets are publicly accessible on the official website [https://covid19.who.int/] (15 December 2022) and are provided in Appendix A. The required calculations were carried out via the R programme.

The following are some of the outcomes. Based on the findings shown in Tables 6–12, we are able to draw the conclusion that the new-PFD is superior to all of its rivals. It is clear that the new-PFD is preferable since it had the lowest K-S values and the greatest p-values. In addition, Figures 3–9 exhibit fitted versions of the pdf, cdf, PP, sf, TTT, and box plots for the new-PFD for each of the seven COVID-19 mortality data sets, respectively. These figures pertain to the new-PFD.

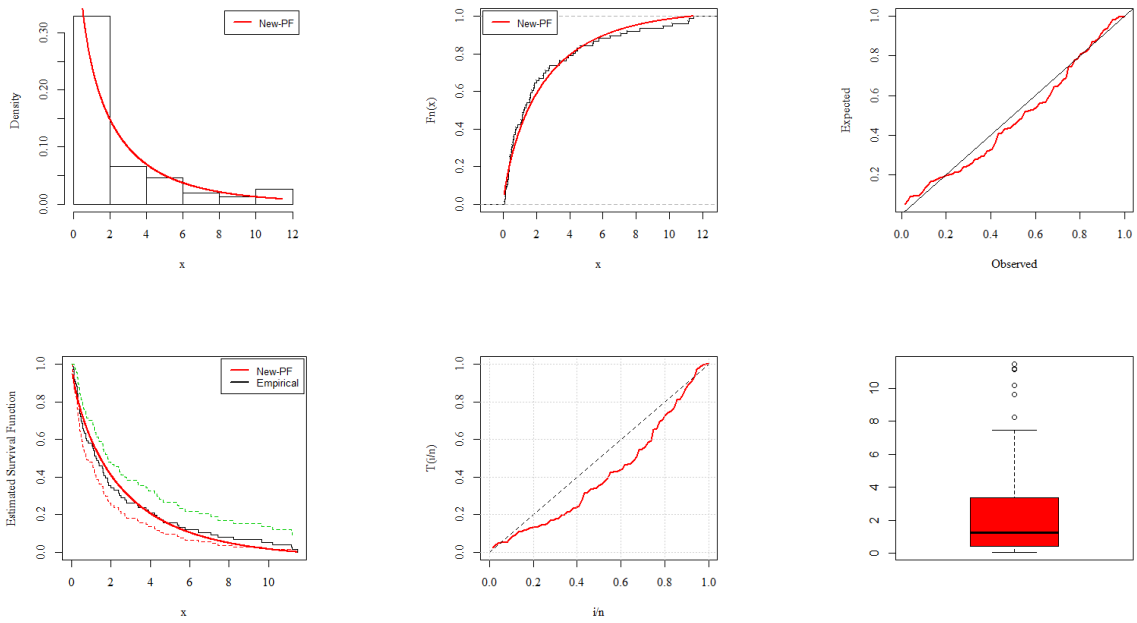

Figure 3. Fitted Curves For United Kingdom Mortality Rate (15 April to 30 June 2020).

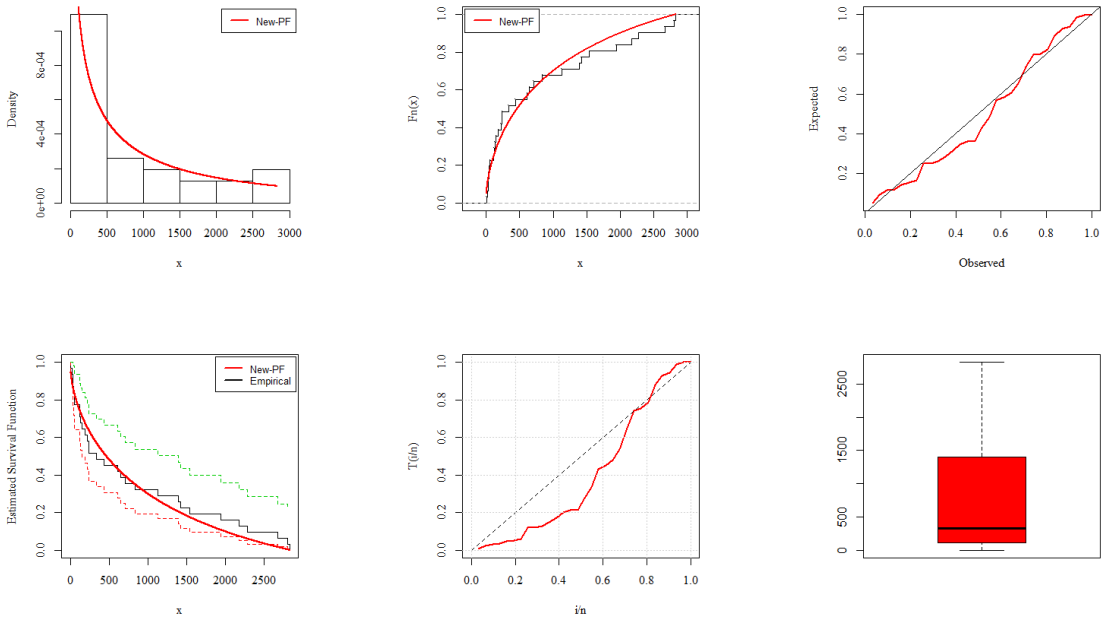

Figure 4. Fitted Curves For Europe Mortality Rate (1 March to 30 March).

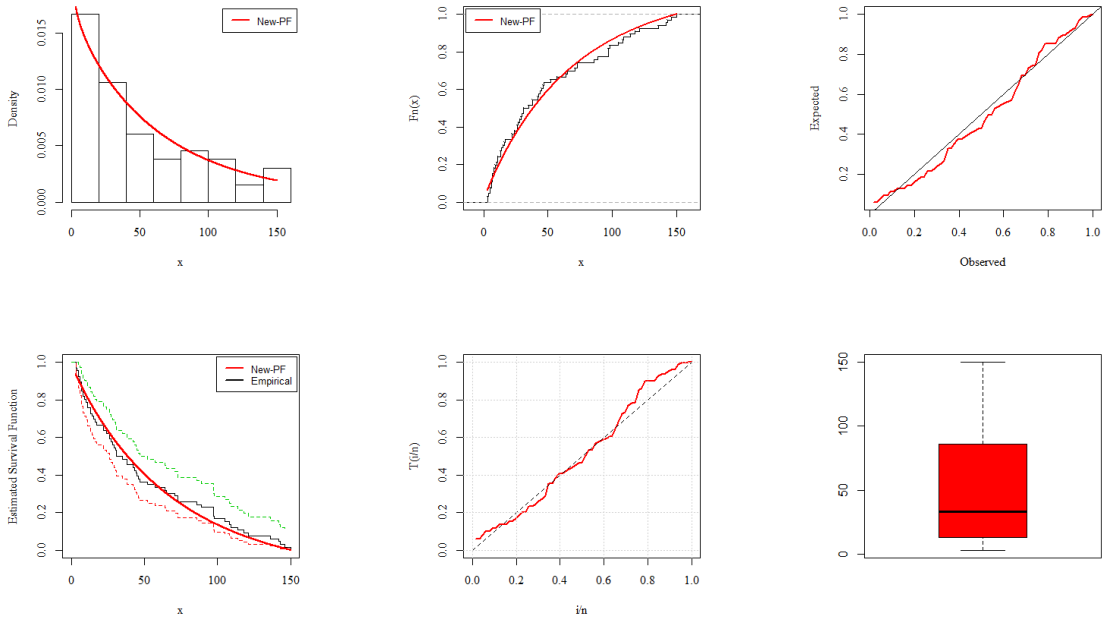

Figure 5. Fitted Curves For China Mortality Rate (23 January to 28 January).

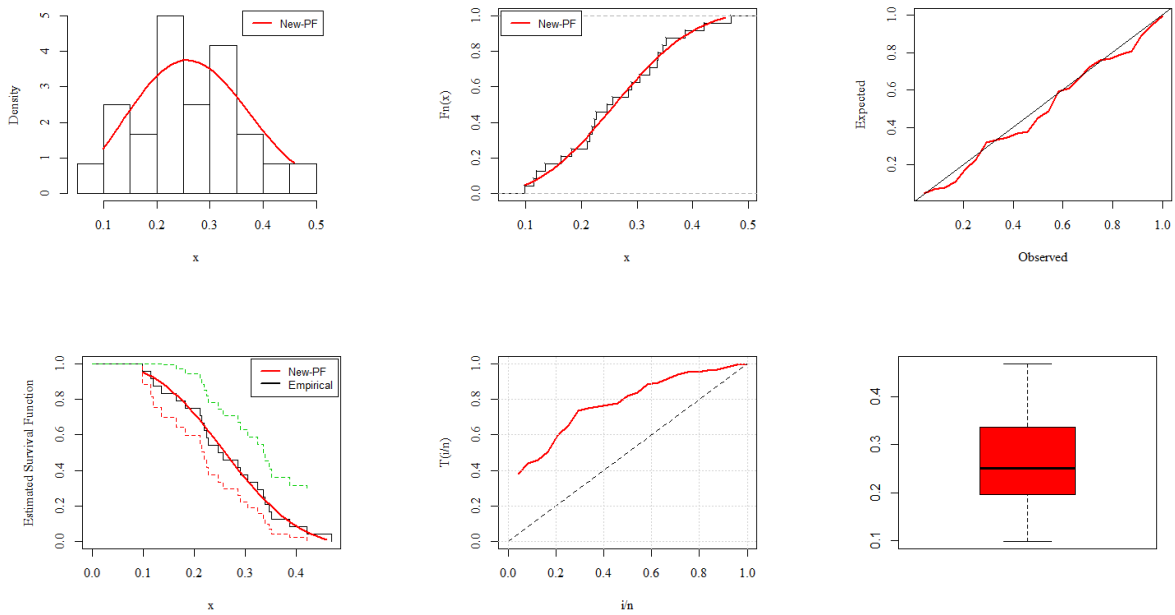

Figure 6. Fitted Curves For United Kingdom Mortality Rate (15 October to 7 November 2020).

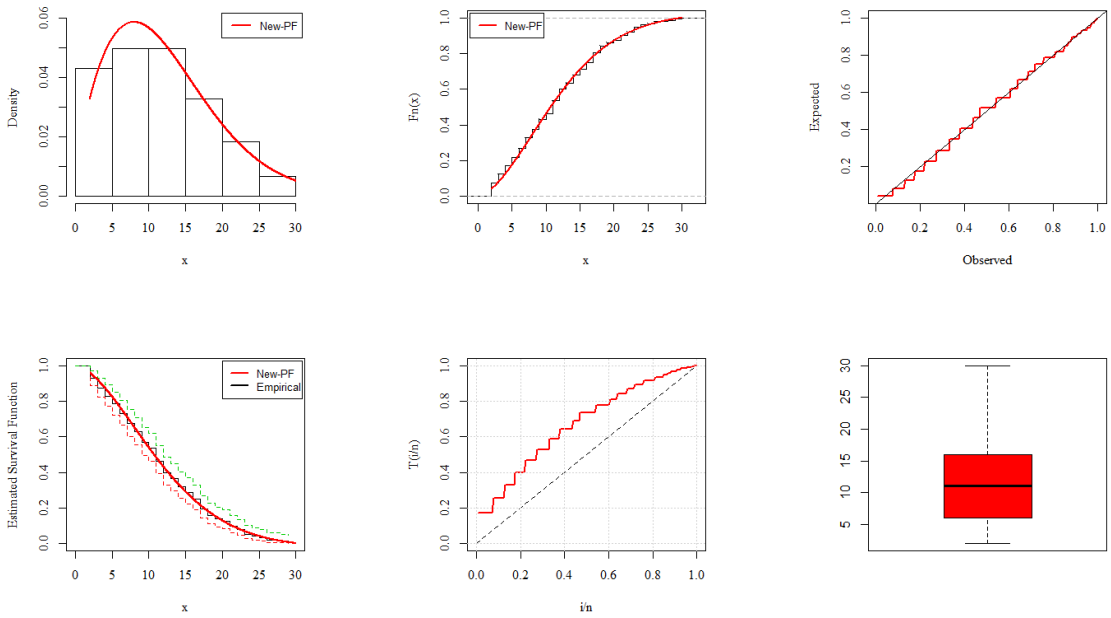

Figure 7. Fitted Curves for Nepal Mortality Rate (23 January 2020 to 24 December 2020).

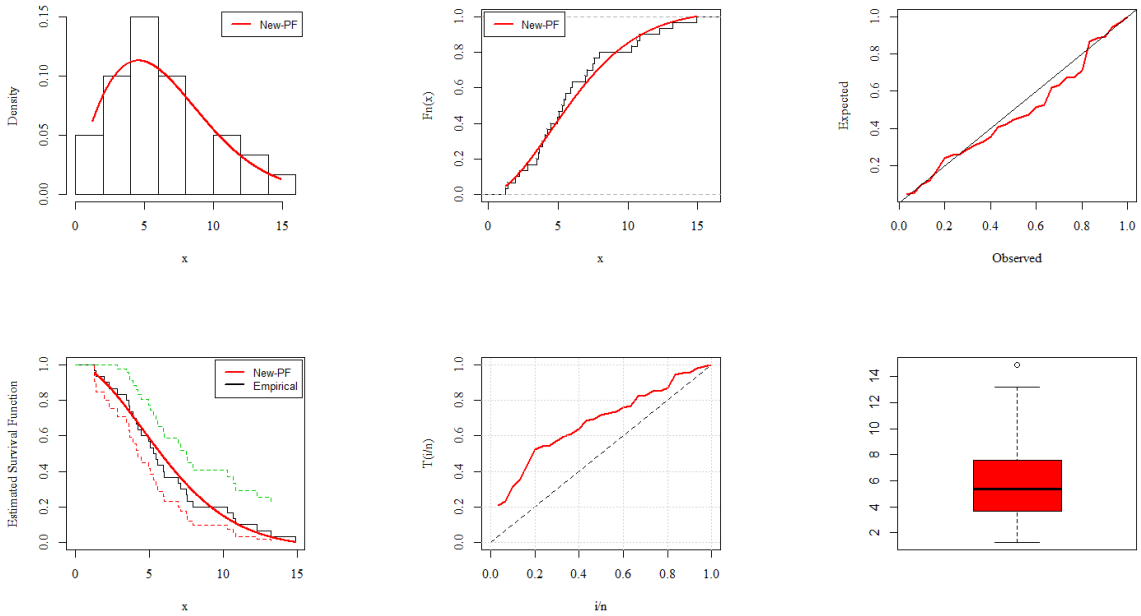

Figure 8. Fitted Curves for Netherland Mortality Rate (31 March 2020 to 30 April 2020).

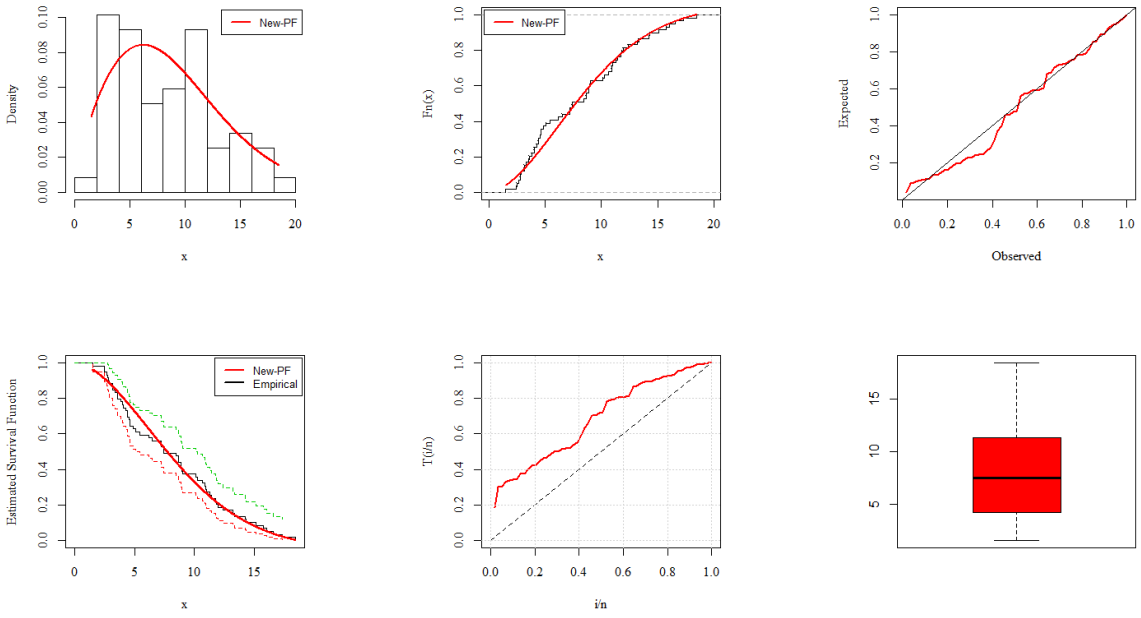

Figure 9. Fitted Curves for Italy Mortality Rate (27 February 2020 to 27 April 2020).

7. Summary and Conclusions

We came up with the idea for a completely new, continuously generated (G) family that is better and more versatile, and we called it the new-G family of distributions. Its mathematical properties, such as cdf, pdf, sf, hrf, asymptotic, OS, and related measures of entropy, have been thoroughly discussed. We investigate every conceivable form that the new-PFD pdf and hrf may have for a variety of parameter combinations, which allows for a greater degree of flexibility in the way it models COVID-19 mortality data. The increasing, decreasing, and bathtub-shaped behaviour of the pdf and hrf of the new-PFD are all represented by flexible forms in a simple and concise manner. In addition, using a full sample as a foundation, we generated random samples to use in our simulation study. From Tables 2–5, we were able to draw the conclusion that all estimates have the consistency property and all estimation methods performed well. We also performed an analysis on the COVID-19 mortality data related to United Kingdom, Europe, China, Nepal,

Netherlands, and Italy, in order to determine the advantages that the proposed new-PFD model has over some of its rivals. Our findings indicate that the new-PFD is a better fit for the data than the distributions that were used in the competing models. In addition to this, we drew the fitted pdf, cdf, PP, and sf plots for the new-PFD for each of the seven COVID-19 mortality data sets, in corresponding order.

We consider that better results can be achieved in COVID-19 mortality data set analysis through the use of the new family because it is more flexible and better able to model the complex patterns of spread and variation in the data. The new family has several characteristics that make them well-suited for modelling COVID-19 mortality data, such as the ability to model heavy tails, skewness, and multimodality, which are often observed in COVID-19 mortality data sets. Additionally, the new family is able to capture the dynamic nature of the spread of the virus, which is critical for understanding the effectiveness of containment measures. These are the reasons why the new family is considered a better model for COVID-19 mortality data set analysis.

8. Future Recommendations

We would be glad to let the researchers have a chance to find out more about what we are doing. Thus, to avoid a lengthy wait for mortality, we suggest instead addressing the proposed study on the censored sample of COVID-19 infections. Furthermore, we want to include it into other regression models to forecast future rates of infection and death across many nations, and to expand upon the proposed work to develop a time series model for the most common diseases. Furthermore, the new family can be used to estimate the probability of large outbreaks and predict the future spread of the virus.

Author Contributions: Methodology, A.S.A.; Validation, M.M.A.E.-R.; Investigation, A.S.A.; Resources, M.M.A.E.-R. All authors have read and agreed to the published version of the manuscript.

Funding: This research received no external funding.

Data Availability Statement: All data exists in the paper with references.

Conflicts of Interest: There are no conflict of interest for any of the authors.

Appendix A

The following data is discussed in the numerical study.

Application I: United Kingdom COVID-19 Mortality Rate

0.0587, 0.0863, 0.1165, 0.1247, 0.1277, 0.1303, 0.1652, 0.2079, 0.2395, 0.2751, 0.2845, 0.2992, 0.3188, 0.3317, 0.3446, 0.3553, 0.3622, 0.3926, 0.3926, 0.4110, 0.4633, 0.4690, 0.4954, 0.5139, 0.5696, 0.5837, 0.6197, 0.6365, 0.7096, 0.7193, 0.7444, 0.8590, 1.0438, 1.0602, 1.1305, 1.1468, 1.1533, 1.2260, 1.2707, 1.3423, 1.4149, 1.5709, 1.6017, 1.6083, 1.6324, 1.6998, 1.8164, 1.8392, 1.8721, 1.9844, 2.1360, 2.3987, 2.4153, 2.5225, 2.7087, 2.7946, 3.3609, 3.3715, 3.7840, 3.9042, 4.1969, 4.3451, 4.4627, 4.6477, 5.3664, 5.4500, 5.7522, 6.4241, 7.0657, 7.4456, 8.2307, 9.6315, 10.1870, 11.1429, 11.2019, 11.4584.

Application II: Europe COVID-19 Mortality Rate

6, 18, 29, 28, 47, 55, 40, 150, 129, 184, 236, 237, 336, 219, 612, 434, 648, 706, 838, 1129, 1421, 118, 116, 1393, 1540, 1941, 2175, 2278, 2824, 2803, 2667.

Application III: China COVID-19 Mortality Rate

8, 16, 15, 24, 26, 26, 38, 43, 46, 45, 57, 64, 65, 73, 73, 86, 89, 97, 108, 97, 146, 121, 143, 142, 105, 98, 136, 114, 118, 109, 97, 150, 71, 52, 29, 44, 47, 35, 42, 31, 38, 31, 30, 28, 27, 22, 17, 22, 11, 7, 13, 10, 14, 13, 11, 8, 3, 7, 6, 9, 7, 4, 6, 5, 3, 5.

Application IV: United Kingdom COVID-19 Mortality Rate

0.2240, 0.2189, 0.2105, 0.2266, 0.0987, 0.1147, 0.3353, 0.2563, 0.2466, 0.2847, 0.2150, 0.1821, 0.1200, 0.4206, 0.3456, 0.3045, 0.2903, 0.3377, 0.1639, 0.1350, 0.3866, 0.4678, 0.3515, 0.3232.

Application V: Nepal COVID-19 Mortality Rate

2, 2, 2, 2, 2, 2, 3, 2, 3, 3, 4, 2, 5, 5, 3, 2, 4, 4, 8, 4, 4, 3, 2, 3, 7, 6, 6, 11, 9, 3, 8, 7, 11, 8, 12, 12, 14, 7, 11, 12, 6, 14, 9, 9, 11, 6, 6, 5, 5, 14, 9, 15, 11, 8, 4, 7, 11, 10, 16, 2, 7, 17, 6, 8, 10, 4, 10, 7, 11, 11, 8, 7, 19, 9, 15, 12, 10, 14, 22, 9, 18, 12, 19, 21, 12, 12, 18, 8, 26, 21, 17, 13, 5, 15, 14, 11, 17, 16, 17, 23, 24, 20, 30, 18, 18, 17, 21, 18, 22, 26, 15, 13, 13, 6, 9, 17, 12, 17, 22, 7, 16, 16, 24, 28, 23, 23,19, 25, 29, 21, 9, 13, 16, 10, 17, 20, 23, 14, 12, 11, 15, 9, 18, 14, 13, 6, 16, 12, 11, 7, 3, 5, 5.

Application VI: Netherland COVID-19 Mortality Rate

14.918, 10.656, 12.274, 10.289, 10.832, 7.099, 5.928, 13.211, 7.968, 7.584, 5.555, 6.027, 4.097, 3.611, 4.960, 7.498, 6.940, 5.307, 5.048, 2.857, 2.254, 5.431, 4.462, 3.883, 3.461, 3.647, 1.974, 1.273, 1.416, 4.235.

Application VII: Italy COVID-19 Mortality Rate

4.571, 7.201, 3.606, 8.479, 11.410, 8.961, 10.919, 10.908, 6.503, 18.474, 11.010, 17.337, 16.561, 13.226, 15.137, 8.697, 15.787, 13.333, 11.822, 14.242, 11.273, 14.330, 16.046, 11.950, 10.282, 11.775, 10.138, 9.037, 12.396, 10.644, 8.646, 8.905, 8.906, 7.407, 7.445, 7.214, 6.194, 4.640, 5.452, 5.073, 4.416, 4.859, 4.408, 4.639, 3.148, 4.040, 4.253, 4.011, 3.564, 3.827, 3.134, 2.780, 2.881, 3.341, 2.686, 2.814, 2.508, 2.450, 1.518.

References

1. Dallas, A.C. Characterizing the Pareto and power distributions. *Ann. Math. Stat.* **1976**, *28*, 491–497. [CrossRef]
2. Saran, J.; Pandey, A. Estimation of parameters of power function distribution and its characterization by the kth record values. *Statistica.* **2004**, *14*, 523–536.
3. Zaka, A.; Akhter, A.S.; Jabeen, R. The new reflected power function distribution: Theory, simulation & application. *AIMS Math.* **2020**, *5*, 5031–5054.
4. Tahir, M.H.; Alizadeh, M.; Mansoor, M.; Cordeiro, G.M.; Zubair, M. The Weibull-power function distribution with applications. *Hacet. J. Math. Stat.* **2016**, *45*, 245–265. [CrossRef]
5. Ahsan-ul-Haq, M.; Butt, N.S.; Usman, R.M.; Fattah, A.A. Transmuted power function distribution. *Gazi Univ. J. Sci.* **2016**, *29*, 177–185.
6. Okorie, I.E.; Akpanta, A.C.; Ohakwe, J.; Chikezie, D.C. The modified power function distribution. *Cogent Math.* **2017**, *4*, 1319592. [CrossRef]
7. Hassan, A.S.; Assar, S.M. A new class of power function distribution: Properties and applications. *Ann. Data Sci.* **2021**, *8*, 205–225. [CrossRef]
8. Meniconi, M.; Barry, D. The power function distribution: A useful and simple distribution to assess electrical component reliability. *Microelectron. Reliab.* **1996**, *36*, 1207–1212. [CrossRef]
9. Marshall, A.W.; Olkin, I. A new method for adding a parameter to a family of distributions with application to the exponential and Weibull families. *Biometrika* **1997**, *84*, 641–652. [CrossRef]
10. Shaw, W.T.; Buckley, I.R. Alchemy of Probability Distributions: Beyond Gram-Charlier and Cornish-Fisher Expansions, and Skewed-kurtotic Normal Distribution from a Rank Transmutation Map. *arXiv* **2009**, arXiv:0901.0434.
11. Eugene, N.; Lee, C.; Famoye, F. Beta-normal distribution and its applications. *Commun. Stat.-Theory Methods* **2002**, *31*, 497–512. [CrossRef]
12. Pourreza, H.; Jamkhaneh, E.B.; Deiri, E. A family of Gamma-generated distributions: Statistical properties and applications. *Stat. Methods Med. Res.* **2021**, *30*, 1850–1873. [CrossRef]
13. Cordeiro, G.M.; de Castro, M. A new family of generalized distributions. *J. Stat. Comput. Simul.* **2011**, *81*, 883–898. [CrossRef]
14. Alzaatreh, A.; Lee, C.; Famoye, F. A new method for generating families of continuous distributions. *Metron* **2013**, *71*, 63–79. [CrossRef]
15. Bourguignon, M.; Silva, R.B.; Cordeiro, G.M. The Weibull-G family of probability distributions. *Data Sci. J.* **2014**, *12*, 53–68. [CrossRef]
16. Cordeiro, G.M.; Alizadeh, M.; Diniz Marinho, P.R. The type I half-logistic family of distributions. *J. Stat. Comput. Simul.* **2016**, *86*, 707–728. [CrossRef]
17. Al-Shomrani, A.; Arif, O.; Shawky, A.; Hanif, S.; Shahbaz, M.Q. Topp–Leone family of distributions: Some properties and application. *Pak. J. Stat. Oper. Res.* **2016**, *12*, 443–451. [CrossRef]
18. Al Mutairi, A.; Iqbal, M.Z.; Arshad, M.Z.; Afify, A.Z. A New Class of the Power Function Distribution: Theory and Inference with an Application to Engineering Data. *J. Math.* **2022**, *2022*, 1206254. [CrossRef]
19. Al-Babtain, A.A.; Gemeay, A.M.; Afify, A.Z. Estimation methods for the discrete Poisson-Lindley and discrete Lindley distributions with actuarial measures and applications in medicine. *J. King Saud Univ. Sci.* **2021**, *33*, 101224. [CrossRef]
20. Liu, X.; Ahmad, Z.; Gemeay, A.M.; Abdulrahman, A.T.; Hafez, E.H.; Khalil, N. Modeling the survival times of the COVID-19 patients with a new statistical model: A case study from China. *PLoS ONE* **2021**, *16*, e0254999. [CrossRef] [PubMed]

21. Nagy, M.; Almetwally, E.M.; Gemeay, A.M.; Mohammed, H.S.; Jawa, T.M.; Sayed-Ahmed, N.; Muse, A.H. The new novel discrete distribution with application on covid-19 mortality numbers in Kingdom of Saudi Arabia and Latvia. *Complexity* **2021**, *2021*, 7192833. [CrossRef]
22. Hossam, E.; Abdulrahman, A.T.; Gemeay, A.M.; Alshammari, N.; Alshawarbeh, E.; Mashaqbah, N.K. A novel extension of Gumbel distribution: Statistical inference with covid-19 application. *Alex. Eng. J.* **2022**, *61*, 8823–8842. [CrossRef]
23. Riad, F.H.; Alruwaili, B.; Gemeay, A.M.; Hussam, E. Statistical modeling for COVID-19 virus spread in Kingdom of Saudi Arabia and Netherlands. *Alex. Eng. J.* **2022**, *61*, 9849–9866. [CrossRef]
24. Alsuhabi, H.; Alkhairy, I.; Almetwally, E.M.; Almongy, H.M.; Gemeay, A.M.; Hafez, E.H.; Aldallal, R.A.; Sabry, M. A superior extension for the Lomax distribution with application to Covid-19 infections real data. *Alex. Eng. J.* **2022**, *61*, 11077–11090. [CrossRef]
25. Meriem, B.; Gemeay, A.M.; Almetwally, E.M.; Halim, Z.; Alshawarbeh, E.; Abdulrahman, A.T.; Abd El-Raouf, M.M.; Hussam, E. The Power XLindley Distribution: Statistical Inference, Fuzzy Reliability, and COVID-19 Application. *J. Funct. Spaces* **2022**, *2022*, 9094078. [CrossRef]
26. Abdul-Moniem, I.B. The Kumaraswamy power function distribution. *J. Stat. Appl. Pro.* **2017**, *6*, 81–90. [CrossRef]
27. Tahir, M.H.; Cordeiro, G.M.; Alizadeh, M.; Mansoor, M.; Zubair, M.; Hamedani, G.G. The odd generalized exponential family of distributions with applications. *JSDA* **2015**, *2*, 1–28. [CrossRef]
28. Hassan, A.S.; Nassr, S.G. A new generalization of power function distribution: Properties and estimation based on censored samples. *Thail. Stat.* **2020**, *18*, 215–234.
29. Okorie, I.E.; Akpanta, A.C.; Ohakwe, J.; Chikezie, D.C.; Onyemachi, C.U.; Rastogi, M.K. Zero-truncated Poisson-power function distribution. *Ann. Data Sci.* **2021**, *8*, 107–129. [CrossRef]
30. Okorie, I.E.; Akpanta, A.C.; Ohakwe, J. Marshall-Olkin extended power function distribution. *FJPS* **2017**, *5*, 16–29.